The Rise and Fall of Pu‘u ‘Ō‘ō Cone, 1983–2002

By Christina Heliker, Jim Kauahikaua, David R. Sherrod, Michael Lisowski, *and* Peter F. Cervelli

Abstract

The Pu‘u ‘Ō‘ō-Kūpaianaha eruption of Kīlauea Volcano, Hawai‘i, began on January 3, 1983. From June 1983 through June 1986, 44 episodes of high fountaining at the Pu‘u ‘Ō‘ō vent constructed a complex basaltic cone, 255 m high and 1.4 km wide at its base, composed of lava flows, agglutinated spatter, and cinder, with an asymmetric shape determined largely by the prevailing trade winds. The steeper slope (36°) on the west side of the cone was controlled by unconsolidated cinder and agglutinated spatter, and the gentler slope (8°) on the east side by lava flows. These two sectors of the cone were separated by transitional zones of rootless spatter flows. At its maximum size, the volume of the cone was ~136x10^6 m^3 (dense-rock equivalent, 67x10^6 m^3) and composed about 20 percent of the total volume of eruptive deposits produced during the 3 years of its growth.

In July 1986, the eruption shifted 3 km downrift to a new vent, Kūpaianaha, which became the locus of activity for the next 5½ years. Episodic collapse from mid-1987 through 1988 resulted in a central crater, 180 m deep and 200 m wide, at Pu‘u ‘Ō‘ō. The elevation of the crater floor stabilized at about the same elevation as the Kūpaianaha lava pond, and a lava pond appeared intermittently in the new crater of Pu‘u ‘Ō‘ō.

In February 1992, Kūpaianaha stopped erupting, and the activity returned to Pu‘u ‘Ō‘ō, where a series of flank vents on the west and southwest sides of the cone have been erupting ever since. The west wall of the cone was gradually undermined by shallow subsurface magma movement associated with flank vents, and collapse pits began to form high on the west flank of the cone in 1993. In January 1997, the magmatic system beneath Pu‘u ‘Ō‘ō was depressurized by an intrusion and a brief fissure eruption 4 km uprift. The crater floor dropped 150 m, and the west wall of the cone collapsed, removing 13x10^6 m^3 of material and enlarging the elliptical crater to 240 by 400 m. The cumulative volume of crater and west-wall collapse since 1987 is 28x10^6 m^3. In addition to catastrophic collapse, the cone is undergoing long-term subsidence. Repeated surveys of bench marks on the cone recorded 63 to 83 cm/yr of subsidence near the crater from 1998 to 2002.

Recent geodetic data from borehole tiltmeters on and near the cone indicate the presence of a deformation source less than 400 m below the preeruption surface. Gravity measurements suggest that the cone is underlain by an elongate zone, parallel to the rift zone, with a density contrast of 0.5 g/cm^3 relative to the surrounding rock. We have modeled the gravity data as a low-density zone, approximately 500 m wide, 1,500 m long, and 300 m thick, occupying a volume 70 to 370 m below the preeruption surface; this low-density zone probably represents brecciated rock laced with magma-filled fractures.

Introduction

The ongoing Pu‘u ‘Ō‘ō-Kūpaianaha eruption (fig. 1), which began in January 1983, is the longest lived eruption on Kīlauea’s rift zones in more than 500 years. Monitoring this eruption has provided ample opportunity to witness catastrophic changes in the landscape on a time scale from days to months. The most striking landform created during this prolonged eruption is Pu‘u ‘Ō‘ō, a basaltic cone composed of cinder, agglutinated spatter, and lava flows. Constructed during 3 years of episodic high lava fountaining, the cone grew to a height of 255 m above the pre-1983 surface. By 1986, Pu‘u ‘Ō‘ō was the most prominent vent structure on either rift zone of Kīlauea, more than 140 m higher than any other cone on the volcano.

Studies of complex basaltic cones (those not composed predominantly of cinder) are rare, and, with the exception of an overview by Head and Wilson (1989), the contribution of rootless agglutinated-spatter flows to basaltic vent structures is little noted in the literature. Since the late 1990s, however, basaltic and andesitic rootless spatter flows have been the focus of studies at Izu-Oshima Volcano (Sumner, 1998) and Asama Volcano (Maya Yasui and Takehiro Koyaguchi, written commun., 2002) in Japan and at Vulcan cone, part of the basaltic Albuquerque Volcanoes, in New Mexico (Smith and others, 1999). These recent studies highlight the need for better documentation of such features, particularly where the eruption is witnessed.

Both the duration and scale of the collapse of Pu‘u ‘Ō‘ō are unique in the recorded history of Kīlauea. The ongoing collapse of the crater and west flank of the cone has resulted from two processes: (1) short-term events that abruptly divert magma from the eruption site, depressurize the magmatic system, and trigger catastrophic collapse; and (2) long-term downcutting by the lava tubes leading from the flank vents that has progressively undermined the west flank of the cone.

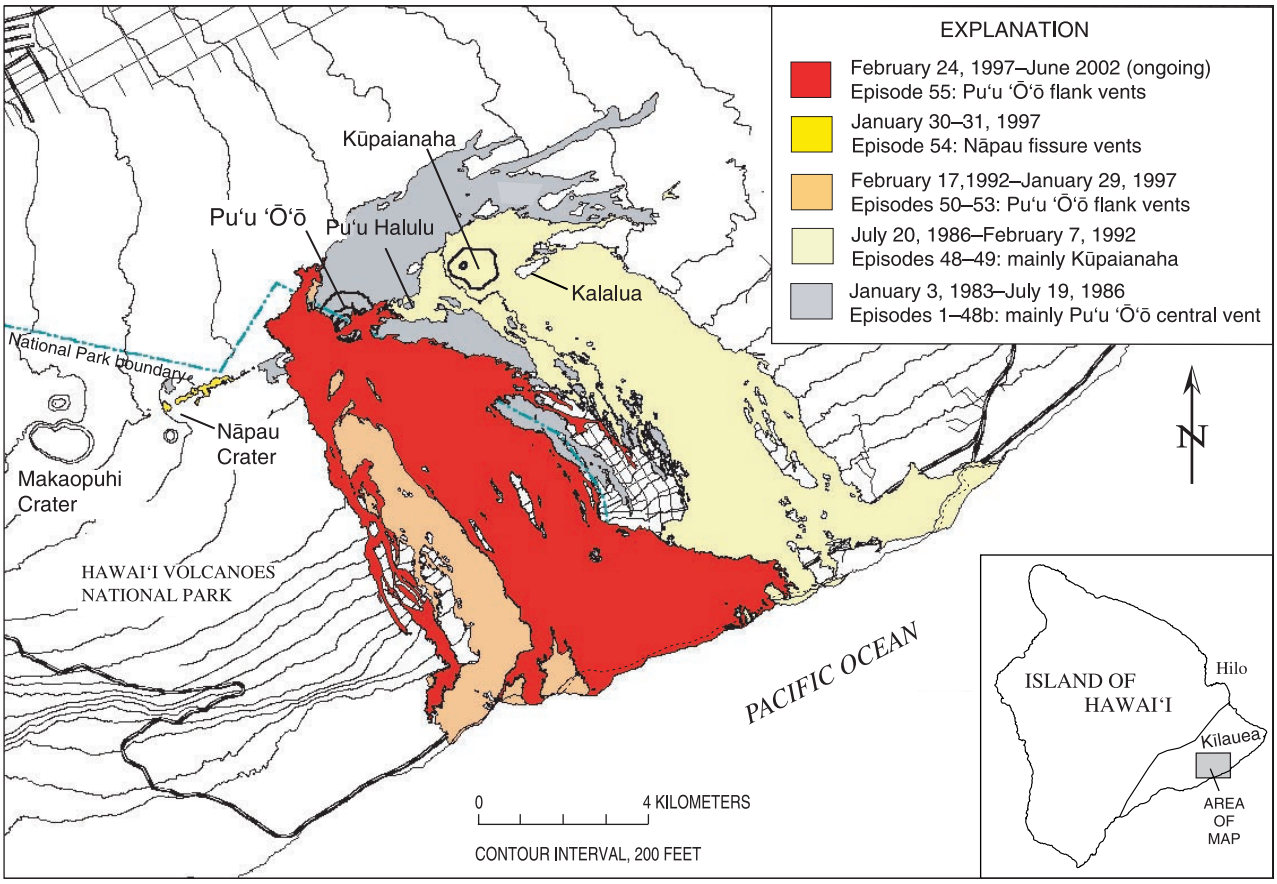

Figure 1. Kīlauea Volcano, Island of Hawai‘i, showing location of Pu‘u ‘Ō‘ō-Kūpaianaha eruption site on east rift zone and lava flows emplaced during eruptive episodes.

Recently obtained gravity and geodetic data, interpreted in the light of the ongoing collapse and the growing number of flank vents, give us a better understanding of the shallow magmatic system beneath Pu‘u ‘Ō‘ō.

The scope of this chapter is limited to those events that bear directly on the growth and later collapse of the Pu‘u ‘Ō‘ō cone. For a full chronology of the eruption, see Heliker and Mattox (this volume).

The Rise of Pu‘u ‘Ō‘ō, June 1983–July 1986

How the Cone Got Its Shape

Within 6 months of its onset in January 1983, the eruption had localized at the Pu‘u ‘Ō‘ō vent (fig. 1). By mid-1984, the activity had settled into a pattern of brief (<24 hour) eruptive episodes, separated by repose periods averaging 25 days in length (George Ulrich and others, The Pu‘u ‘Ō‘ō-Kūpaianaha eruption of Kīlauea Volcano, Hawaii: episodes 21 through 48, U.S. Geological Survey Open-File Report, in preparation). Over the next 3 years, 44 episodes of high fountaining built a cinder-and-spatter cone, 255 m high and 1.4 km in diameter at its base (fig. 2).

Within its first few months, the cone developed an asymmetric shape, because the prevailing northeasterly trade winds deflected most of the tephra to the southwest side of the vent. This asymmetry became more pronounced in mid-1984, when maximum fountain heights increased from less than 250 to 300–470 m, with a corresponding increase in the volume of tephra deposits. The summit gained as much as 27 m in height during each high fountaining episode and, by July 1986, stood 86 m higher than the vent (fig. 3). The southwest side of the cone rose like a backstop behind the fountains.

The rapid increase in cone height slowed markedly after October 1985 (table 1; fig. 4), because fountain heights were substantially lower and southwesterly winds prevailed during half of the remaining high-fountaining episodes. The vent continued to increase in elevation, however, which may have contributed to the end of high fountaining at Pu‘u ‘Ō‘ō in mid-1986.

By December 1983, the Pu‘u ‘Ō‘ō vent had consolidated into a single circular opening approximately 20 m in diameter. The conduit below the vent was a vertical pipe of constant diameter, visible to approximately 50-m depth. During its first year, the vent was situated in a shallow crater. Lava overflowed from the crater into spillways, which had been established on the east side of the cone during its first 6 months (Wolfe and others, 1988). Generally, the lava exited through one or two spillways that persisted through several eruptive

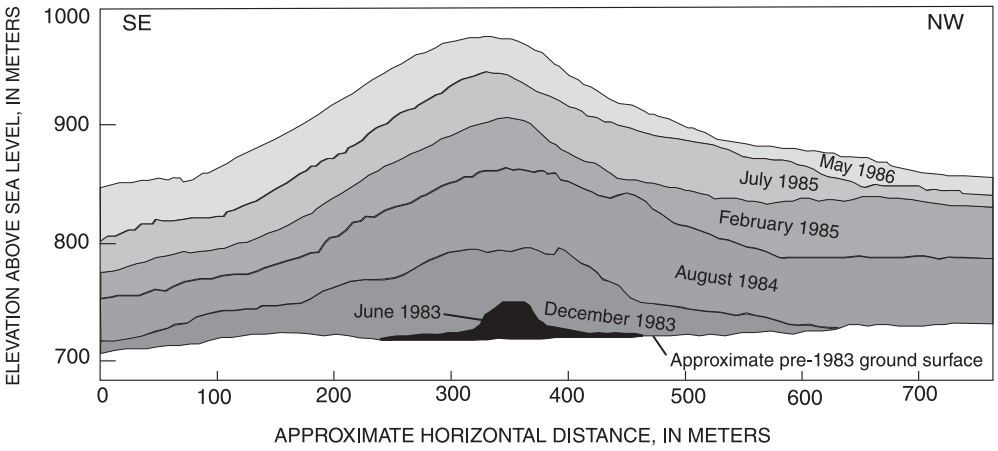

Figure 2. Profiles showing growth of Pu‘u ‘Ō‘ō cone, June 1983 through May 1986, traced from photographs taken from Pu‘u Halulu. Vertical scale constrained by cone-height measurements taken by theodolite at end of each eruptive episode; horizontal scale from topographic surveys. Profiles for June and December 1983 from Wolfe and others (1988).

episodes. After low-level effusion during episode 19 (May 1984), the crater was filled to the level of the spillways (Wolfe and others, 1988), creating an amphitheater opening eastward. The increasing breadth of the fountains flattened the area around the vent, and, by episode 34 (July 1985), a broad ramp sloped from the vent toward the spillways (fig. 5).

By mid-1985, the cone's morphology was firmly established, with lava spillways to the east of the vent and a steep, cinder-covered flank to the west. These two sectors of the cone were separated by transitional zones of rootless spatter flows, partly buried by cinder, on the north and south flanks (fig. 5). The slope of the west (summit) side of the cone, which was controlled by unconsolidated cinder and agglutinated spatter, was 36°, whereas the slope of the east (spillway) side was only 8°.

The Components of the Cone

Lava Flows

The style of the eruption at Pu‘u ‘Ō‘ō changed progressively throughout its first year from low fountains that fed pāhoehoe flows to high fountains that fed ‘a‘ā flows. Episodes 4 through 19 (June 1983–May 1984) were characterized by channeled pāhoehoe flows that spilled from a lava pond at the base of the fountains (Wolfe and others, 1988). These fluid rivers carried most of the lava away from the cone before the flows underwent the transition to ‘a‘ā 1 to 2 km from the vent (Wolfe and others, 1988).

Beginning with episode 20 (June 1984), fountain-fed ‘a‘ā flows became the norm, mainly because fountain heights increased substantially. Maximum fountain heights fluctuated widely in the early Pu‘u ‘Ō‘ō episodes but were rarely more than 250 m. From episodes 20 through 41, however, maximum fountain heights were consistently more than 300 m, and during about half of these episodes, more than 400 m. The flows were fed directly by fallback from the fountains, resulting in lava with a higher viscosity and yield strength, owing to the loss of heat and volatile components during fountaining (Sparks and Pinkerton, 1978). When sustained fountain heights decreased during episodes 42 through 47 in 1986, channeled pāhoehoe flows were observed once again. A similar correlation between fountain height and flow type was documented during the 1961 Askja eruption in Iceland (Sparks and Pinkerton, 1978).

The predominance of ‘a‘ā flows near the vent caused a substantial buildup of the adjacent terrain on the north, east, and south sides of the cone, blurring the distinction between the cone and the surrounding lava-flow field. Lava rivers flowing down the spillways coalesced at the foot of the cone to form broad, thick fans of ‘a‘ā that piled up near the cone for several hours at the beginning of each episode.

Agglutinated Spatter and Rootless Flows

Spatter falling from the fountains fed all of the lava flows erupted during high-fountaining episodes. Although such spatter-fed flows are generally defined as clastogenic rather than coherent (Wolff and Sumner, 2000), this distinction is not useful in the field for Hawaiian eruptions, where complete coalescence of clasts takes place at the base of the fountain. A distinction can be made, however, between channeled flows

Figure 3. Pu‘u ‘Ō‘ō during episode 46, June 2, 1986. Summit is 86 m higher than vent, owing to prevailing trade winds. View southward.

Table 1. The Pu‘u ‘Ō‘ō cone and central-vent heights, measured by theodolite from Pu‘u Halulu at the end of each eruptive episode.

[Horizontal distance to cone determined periodically by electronic distance meter. Data for episodes 4 through 20 from Wolfe and others (1988).]

Date	Episode	Cone height (meters above pre-1983 surface)	Cone height (meters above sea level)	Vent height (meters above pre-1983 surface)	Vent height (meters above sea level)
06/17/83	4	25	744	--	--
12/01/83	12	80	799	--	--
03/04/84	16	100	819	--	--
04/21/84	18	118	837	--	--
05/18/84	19	120	839	--	--
06/08/84	20	130	849	--	--
06/31/84	21	142	861	--	--
07/09/84	22	145	864	--	--
08/21/84	24	150	869	--	--
09/20/84	25	162.5	881.5	--	--
10/28/84	--	157	876	--	--
11/05/84	26	164	883	--	--
11/20/84	27	184	903	--	--
11/28/84	--	167	886	--	--
12/04/84	28	187	906	--	--
12/30/84	--	174	893	135	854
01/04/85	29	201	920	129	848
01/17/85	--	193	912	--	--
02/05/85	30	194	913	133	852
03/15/85	31	206	925	131	850
04/22/85	32	214	933	132	851
04/29/85	--	209	928	--	--
06/13/85	33	212	931	136	855
07/07/85	34	228	947	--	--
08/09/85	35	232	951	--	--
09/03/85	36	242	961	140	859
09/25/85	37	243	962	140	859
10/21/85	38	251	970	141	860
11/29/85	39	250	969	144	863
01/02/86	40	250	969	147	866
01/28/86	41	250	969	148	867
02/23/86	42	250	969	--	--
03/22/86	43	255	974	--	--
04/14/86	44	255	974	154	873
05/08/86	45	255	974	--	--
06/02/86	46	255	974	--	--
06/27/86	47	255	974	169	888
07/19/86	48	255	974	--	--
10/06/88	48	253.5	972.5	--	--
01/17/91	48	236.5	955.5	--	--
09/17/91	48	235.5	954.5	--	--
01/13/92	48	235.5	954.5	--	--
02/02/92	48	234.5	953.5	--	--
03/25/93	53	234	953	--	--
03/04/94	53	234	953	--	--
08/11/95	53	233	952	--	--
06/27/96	53	233	952	--	--
01/09/97	53	232.5	951.5	--	--
01/31/97	54	198	917	--	--
01/18/01	55	189	908	--	--

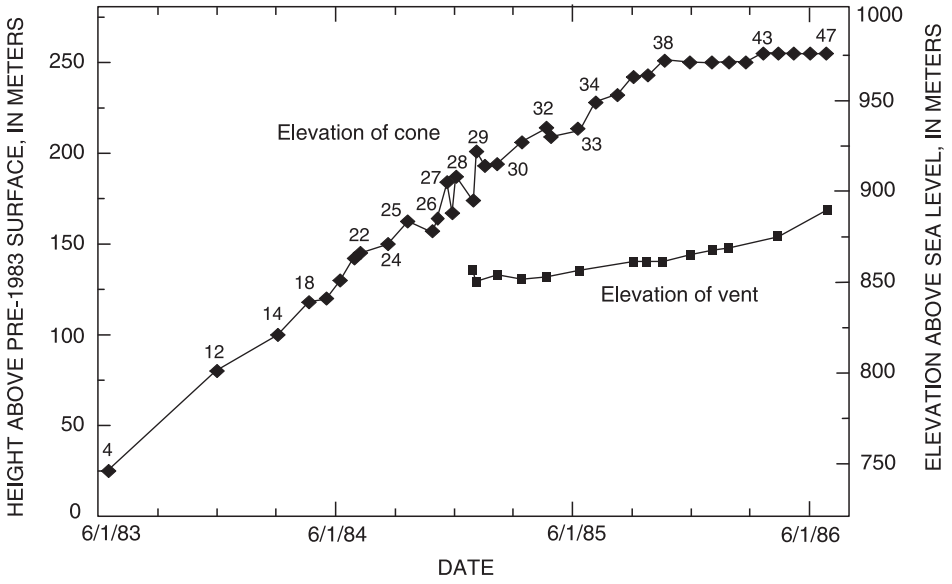

Figure 4. Growth of the Pu‘u ‘Ō‘ō cone during episodes 4 through 47, as determined by theodolite measurements from Pu‘u Halulu. Decreases in cone elevation are due to slumping of agglutinated spatter at summit soon after the end of an eruptive episode. Data from episodes 4 through 20 from Wolfe and others (1988).

fed by continuous fallout from the fountains and rootless flows fed by a discontinuous supply of spatter. Rootless flows are commonly referred to as clastogenic flows at other volcanoes, but we avoid this term to prevent confusion.

By episode 10 (October 1983), most channeled lava flows were funneled through spillways on the east side of the cone. Intense but intermittent spatter fallout on the steep north and south slopes of the cone, however, created thick, broad, rootless flows that extended as far as 3 km from the vent (Wolfe and others, 1988). Rootless flows on the west and southwest sides of the cone were short and stubby because the growing summit blocked deposition on this flank.

Some rootless flows resulted from steady accumulation of spatter near the edge of the fountain; others started after an abrupt change in fountain trajectory quickly slopped a huge load of spatter onto the rim. When fountains were highest, waves of fluid spatter intermittently spilled down the slopes. The largest rootless flows began several hours into a high-fountaining episode, after a substantial volume of agglutinated spatter had accumulated on the upper slopes of the cone.

Many remobilized spatter flows were more than 5 m thick on the upper slopes of the cone. The initial spatter deposits apparently had sufficient yield strength to impede immediate mobilization, probably because of cooling during intermittent deposition. The spatter accumulated and compacted until gravitational stress overcame the yield strength of the massive deposit.

Close to the vent, the larger rootless spatter flows consisted of thick sheets of agglutinate that became deeply fissured as the deposit began to slide (fig. 6)**.** Midway down the cone, where the slope was steepest, the sheets broke apart into a chaotic jumble of truck-size blocks. With continued movement, the blocks split into progressively smaller pieces that slid or rolled downhill; rootless flows that reached the base of the cone fanned out into lobes that resembled a typical ‘a‘ā flow but lacked flow channels (fig. 7).

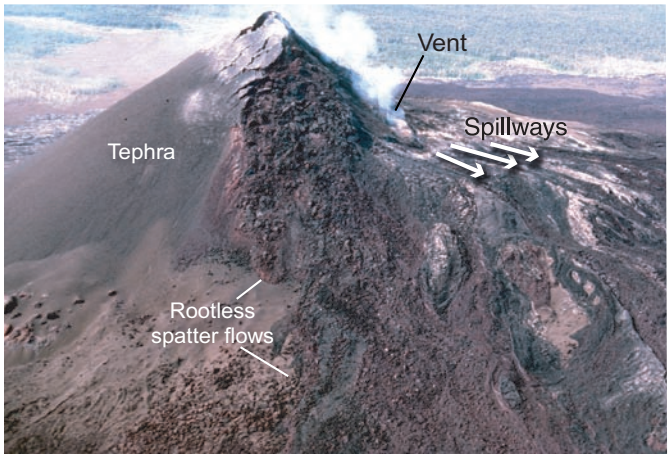

Figure 5. Pu‘u ‘Ō‘ō cone after episode 38. View northward; photograph taken by J.D. Griggs on November 12, 1985.

Figure 6. Agglutinated spatter forms deeply fissured carapace on upper slopes of Pu‘u ‘Ō‘ō cone after episode 29. View northwestward; photograph taken by G.E. Ulrich, on February 1, 1985.

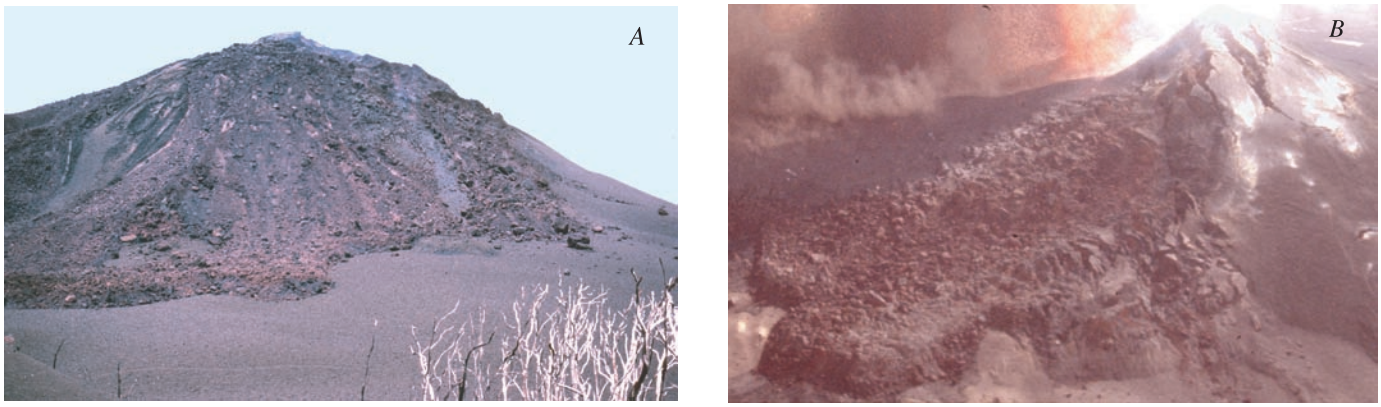

Figure 7. The Pu‘u ‘Ō‘ō cone. *A*, Rootless spatter flows on west side of cone emplaced during episode 33. Relief from top to bottom of flow is about 175 m. Photograph taken June 13, 1985. *B*, Rootless spatter flow on northwest side of cone emplaced during episode 29 (January 1985). Lobe at lower left is 11 m thick. Photograph taken by J.D. Griggs on February 4 1985.

Some rootless flows mobilized entire sectors of the rim or upper slopes of the cone, leaving conspicuous scarps in their wake. Such flows sometimes were reported as cone collapses. This terminology obscures their actual origin, however, because the flows formed during or immediately after high fountaining and mobilized deposits of still-hot agglutinate.

Several rootless flows are still exposed on the cone, although all have been beheaded by widening of the crater. The best-preserved rootless flow formed during episode 45 (May 1986) on the northwest slope of the cone. Transverse fissures, 5 m deep, cut the head of the 30-m-wide flow. Just below the deeply fissured area is an undulating, concave surface where the agglutinate slid as a single mass. At a steep break in slope, the flow broke into large blocks and ploughed aside ridges of cinder and agglutinate blocks as it advanced. Near the flow terminus, 400 m from the rim of the cone, the blocks were reduced to a size typical of ‘a‘ā. Striations are ubiquitous, both on loose blocks and on the slip surfaces that floor the deep fissures at the head of the flow (fig. 8).

Tephra

After episode 33 (June 1985), the cone’s summit, by then 75 m higher than the vent, became a barrier that prevented the thick accumulation of spatter needed to generate large rootless flows. Thereafter, except for small summit-capping rootless flows, the south and west sides of the cone were covered by a smooth blanket of unconsolidated tephra that extended 2 km southwestward of the cone. The tephra consisted predominantly of cinder lapilli but also included bombs of spatter and reticulite, as well as fine Pele’s tears and hair.

During a typical eruptive episode with northeasterly trade winds, 1 to 1.5 m of unconsolidated tephra accumulated at the southwest base of the cone and 4 to 5 m on the upper flanks. A collapse pit that later formed in this area exposed 14 m of unconsolidated tephra, a minimum final thickness of the tephra layers overlying earlier rootless spatter flows in that area.

Theodolite measurements of the cone’s height after each eruptive episode were used to estimate the accumulation rate

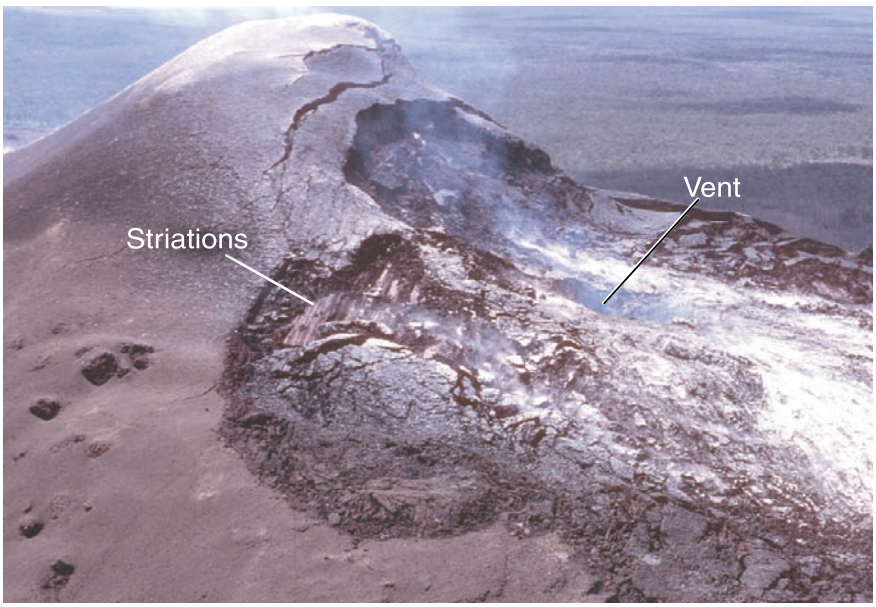

Figure 8. Striated surface on south shoulder of cone, formed by sliding mass of agglutinated spatter during or shortly after episode 30. View northwestward; photograph taken by J.D. Griggs on March 4, 1985.

Figure 9. (facing page) The Pu‘u ‘Ō‘ō crater walls on August 30, 1990. View southwestward; photograph taken by J.D. Griggs.

of fallout deposits. During three episodes, the summit grew more than 20 m in height, and the average instantaneous accumulation rate was 2 to 3 cm per minute—less than the actual rate, both because of compaction and mass flow of tephra from the summit during high fountaining.

After trade-wind-dominated episodes, clean-edged cracks, as much as 10 m wide, formed in the tephra on the summit and shoulders of the cone, parallel to the rim (figs. 5, 7*B*, 8). Observed from the air shortly after fountaining ended, the interiors of these cracks were incandescent. Investigation of similar cracks preserved on the cone reveals that they cut agglutinated deposits, capped by a thin veneer of loose cinder, and are not slumps in unconsolidated tephra. Cinder deposited on the summit and shoulders of the cone was directly exposed to the heat of the lava fountains and may have reheated enough to weld. The deposits subsequently cracked and slid, sometimes leaving striated surfaces above the vent or on the shoulders of the cone (fig. 8).

Cone Stratigraphy

When a large crater formed over the Pu‘u ‘Ō‘ō vent, strata of agglutinated spatter, lava flows, and unconsolidated tephra were exposed. The crater wall beneath the cone’s summit (since removed by collapse) displayed layers of dense gray agglutinated spatter, 1 to 3 m thick, and less dense red to brown agglutinate and unconsolidated tephra, 2 to 8 m thick (fig. 9). The gray agglutinate probably owes its color to a higher degree of compaction that prevented subsequent oxidation.

The red layers thickened beneath the summit and probably represented most of the fallout, whereas the gray layers had a more uniform thickness and were draped over successive summits. Prominent layers beneath the summit could be traced around the south crater wall, where they thinned and pinched out near the east rim. Beneath the east rim, the layers are thinner and include lava flows, as well as agglutinated spatter. Spillway positions are marked by discontinuities in the strata.

A white precipitate that coats the planar faces of the gray agglutinate makes them conspicuous and easy to trace, but the red to brown layers blend together and are impossible to identify individually from a distance. For many years, the crater walls could be viewed only from the rim, and the few available hand specimens were deposited by infrequent explosions that littered the northwest slope of the cone with lithic blocks excavated from the interior of the cone.

Part of the crater-wall stratigraphy became accessible when the west wall of the cone collapsed in 1997 to form the “West Gap” (figs. 10, 11*D*). When examined closely, some of the red units in the north wall of the West Gap prove to be sequences grading upward from 2 to 3-m thick, dark-red, moderately dense agglutinate (0.95–1.90 g/cm^3)

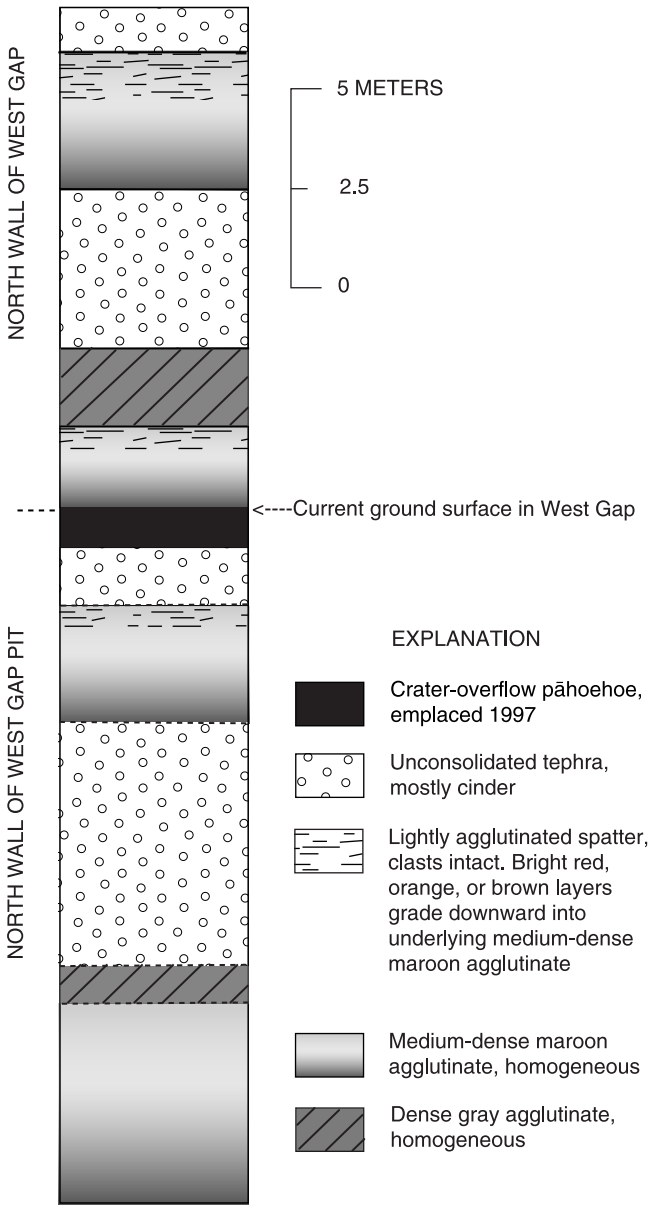

Figure 10. Stratigraphic section of north wall of West Gap in the Pu‘u ‘Ō‘ō cone. Collapse of January 1997 exposed 12.4 m of wall; enlargement of collapse pit at base of wall in September 2000 exposed an additional 17.5 m. Wall of pit is mapped from rim, and so thickness of layers is approximate. Dip of strata, 32°.

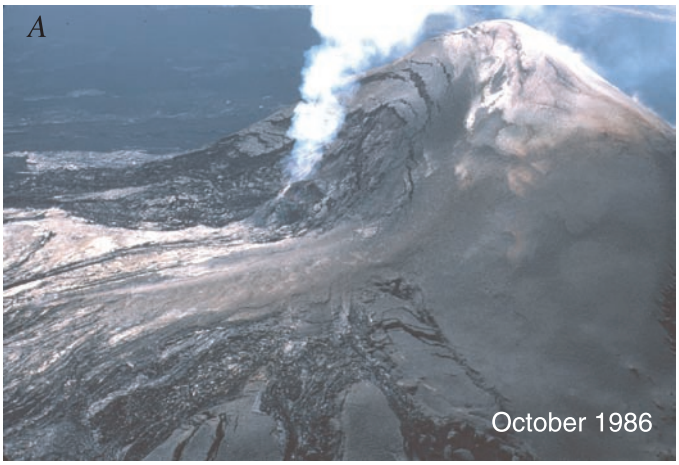

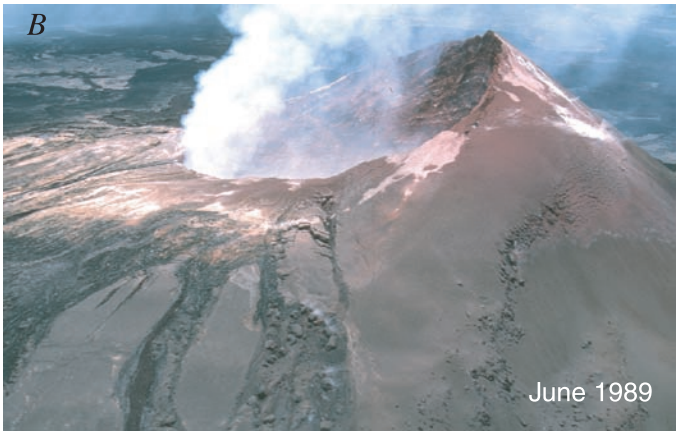

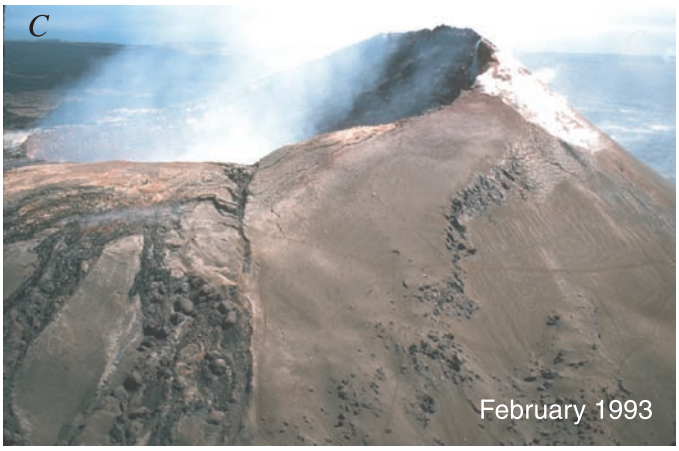

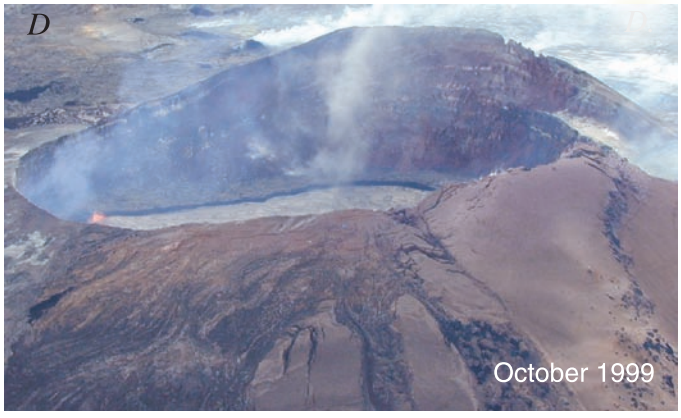

to thin, porous layers oxidized bright orange or red (fig. 10). Similar sequences are visible in rootless spatter flows on the flanks of the cone. The most voluminous component of the agglutinate sequences consists of homogeneous maroon layers with densities of about 1.5 g/cm^3. Clast outlines are rarely visible in outcrop in these layers. The porous layers capping the sequences consist of barely deformed spatter bombs sintered at the contact points with adjacent clasts. The gray agglutinate layer accessible in the wall is homogeneous in color and density (2.3 g/cm^3), except for a thin, dark-red, vesicular top.

The north wall of the West Gap (including the section exposed by an adjacent collapse pit) also includes three layers of unconsolidated tephra, 1.5 to 6 m thick, sandwiched between thick layers of agglutinated spatter (fig. 10). Each of the high fountaining episodes in 1985–86 had about the same duration and eruption rate, and so the widely varying degree of welding at this site apparently resulted from differences in fountain trajectory—which varied by as much as 15° from vertical during some eruptive episodes—and wind direction. These factors determined the size and temperature of the fallout clasts and the rate and continuity of their accumulation.

Some of the thickest gray layers are exposed beneath the southeast rim of the present-day crater, where rootless spatter flows originated during nearly every episode of high fountaining. The densest agglutinate (2.9 g/cm^3) preserved on the surface of the cone forms the basal layer of a rootless flow on the northwest flank. The basal layer was compressed and degassed as thick layers of overlying agglutinate slid across it, leaving behind grooves and striations. The denser gray agglutinate layers in the crater walls, traceable for some distance, may represent basal agglutinate units that were slip surfaces for rootless flows (for example, striated surface, fig. 8).

Volume and Bulk Density of the Cone and Its Components

The maximum volume of the Puʻu ʻŌʻō cone, approximately 136x10^{6}m^3, was estimated by digitizing the contours of the late 1986 (precollapse) cone, then using Geographic Information System (GIS) software to calculate the difference between these and the preeruption digital elevation model (DEM). A bulk density of 1.5 g/cm^3 for the cone, derived from the estimated proportion and density of its various components (table 2), was used to reduce the raw volume to a dense-rock-equivalent (DRE) volume of 67x10^{6}m^3.

Figure 11. Puʻu ʻŌʻō, showing evolution of crater. View southward. *A*, Vent is 20 m wide and topped by small spatter cone in October 1986, after shift in eruption site to Kūpaianaha. *B*, Crater is about 210 m in diameter in June 1989, after 2 years of collapse over central vent. *C*, By February 1993, crater is 240 by 320 m. *D*, Crater and West Gap (to right) in October 1999, after collapse in January 1997 removed west wall of cone. Photographs in figures 11*A* and 11*B* by J.D. Griggs.

Table 2. Estimated density of the Pu‘u ‘Ō‘ō cone and its components.

[Dense-rock equivalent density, 3 g/cm^3. Bulk density of tephra estimated by packing tephra into known volume and weighing it; bulk density of lava based on average of bulk densities for Pu‘u ‘Ō‘ō ‘a‘ā, as determined by D.J. Johnson (Wolfe and others, 1987); bulk density of agglutinated spatter based on average of density measurements on 10 samples, weighted according to estimated proportion of different types of agglutinate.]

Component	Raw volume (10^6 m^3)	Estimated percent	Bulk density (g/cm^3)	Dense-rock-equivalent volume (10^6 m^3)
Unconsolidated tephra	20	15	0.32	2.2
Lava	41	30	2.0	27
Agglutinated spatter	75	55	1.5	38
Totals	136	100		67

Our estimated raw volume is similar to that of Rowland and others (1999), who calculated a volume of 122x10^6 m^3 by subtracting the preeruption DEM volume from an airborne interferometric-radar TOPSAR DEM volume measured in 1993. Though relatively precise, the TOPSAR data have a vertical accuracy no better than ±5 m, owing to the difficulty in matching the vertical datum of pre-1983 topographic maps. Another source of uncertainty is an aspect-ratio distortion—for at least the upper part of the Pu‘u ‘Ō‘ō cone—as judged by our machine contouring of the TOPSAR DEM data provided by S.K. Rowland. A more subjective difference between our method and Rowland’s arises over the difficulty in delineating the cone’s outer boundary, which is abrupt only on the south and west flanks. Thus, the analytical uncertainty for each method is probably about 10 percent.

The estimated DRE volume of the cone is about 20 percent of the total volume of eruptive deposits produced during the 3-year period of cone growth (episodes 4–47). Lava flows predominate in the deposits beyond the base of the cone, along with a very small amount of tephra. Tephra was measured in downwind transects during episodes 25 through 34, the period of highest fountain heights and greatest fallout. During these 10 episodes, tephra volumes (DRE) ranged from 0.8 to 4.1 percent (avg of 1.9 percent) of the total volume of eruptive deposits.

End of Cone Building, July 1986

In July 1986, the conduit beneath Pu‘u ‘Ō‘ō ruptured, and fissures erupted for a day, first on the uprift, then on the downrift, side of the cone. Then, 2 days later, a new fissure opened 3 km downrift of Pu‘u ‘Ō‘ō. This fissure evolved into the Kūpaianaha shield, which became the focus of the eruption for the next 5½ years. During that time, no lava flows issued from Pu‘u ‘Ō‘ō, although ample evidence indicated that it was still linked to the magmatic conduit leading from Kīlauea’s summit reservoir to Kūpaianaha. For a year after the eruption shifted to Kūpaianaha, the Pu‘u ‘Ō‘ō vent remained incandescent, a chimney venting gases from magma on its way to Kūpaianaha. During this period, 500–1,000 t of SO_2 per day were released from Pu‘u ‘Ō‘ō (Elias and others, 1998).

The Fall of Pu‘u ‘Ō‘ō, June 1987 to Present

Central Crater Formation, 1987–92

On June 25, 1987, nearly a year after the eruption shifted to Kūpaianaha, the Pu‘u ‘Ō‘ō vent abruptly collapsed, forming a vertical-walled crater about 100 m deep and 30 to 40 m in diameter. Piecemeal collapse continued to the end of the year, when the new crater was 150 m deep. Lava appeared briefly on the floor of the new crater 3 days after the initial collapse and again at the end of 1987. For the rest of Kūpaianaha’s tenure, active lava was observed intermittently at the bottom of the Pu‘u ‘Ō‘ō crater. The cylindrical crater deepened episodically until December 1988, when it stabilized at a depth of approximately 180 m, which remained more or less constant through mid-1990. The diameter of the crater, about 200 m at the end of 1988, continued to increase gradually (fig. 11).

At the end of 1988, the volume of the Pu‘u ‘Ō‘ō crater was approximately 5.6x10^6 m^3 (table 3). The elevation of active lava on the crater floor was nearly the same as that of the Kūpaianaha lava pond; the feeding conduits at both vents were thus in hydrostatic equilibrium (figs. 12*A*,12*B*). We surmise that the crater formed as material subsided into voids created when the conduit beneath the cone drained and the eruption shifted to Kūpaianaha, 226 m lower in elevation than the Pu‘u ‘Ō‘ō vent.

Eruption Returns to Pu‘u ‘Ō‘ō, February 1992

In mid-1990, the lava pond in the Pu‘u ‘Ō‘ō crater rose to 80 m below the rim as the conduit linking Pu‘u ‘Ō‘ō and Kūpaianaha began to constrict (Mangan and others, 1995; Kauahikaua and others, 1996). Thereafter, a lava pond was nearly always present at the bottom of the crater (fig. 9). As output from Kūpaianaha steadily declined through 1991, activity within the Pu‘u ‘Ō‘ō crater intensified, and the lava pond continued to rise. In November 1991, a fissure eruption

Table 3. (facing page) The Pu‘u ‘Ō‘ō crater’s depths, dimensions, and volume of major crater-collapse events.

[Crater depths, from low point on east rim, estimated by various methods, ranging from estimates made by airborne observers to direct measurements made by lowering cable from the rim (for description, see Heliker and others, 1998a). Measurements in 1992–2002 are generally accurate to within ±5 m except during January–February 1997, with crater at its deepest and floor visible only from the air. Crater dimensions scaled from aerial photographs (asterisks) where available; crater was nearly circular through mid-1989, and so only one dimension is recorded.]

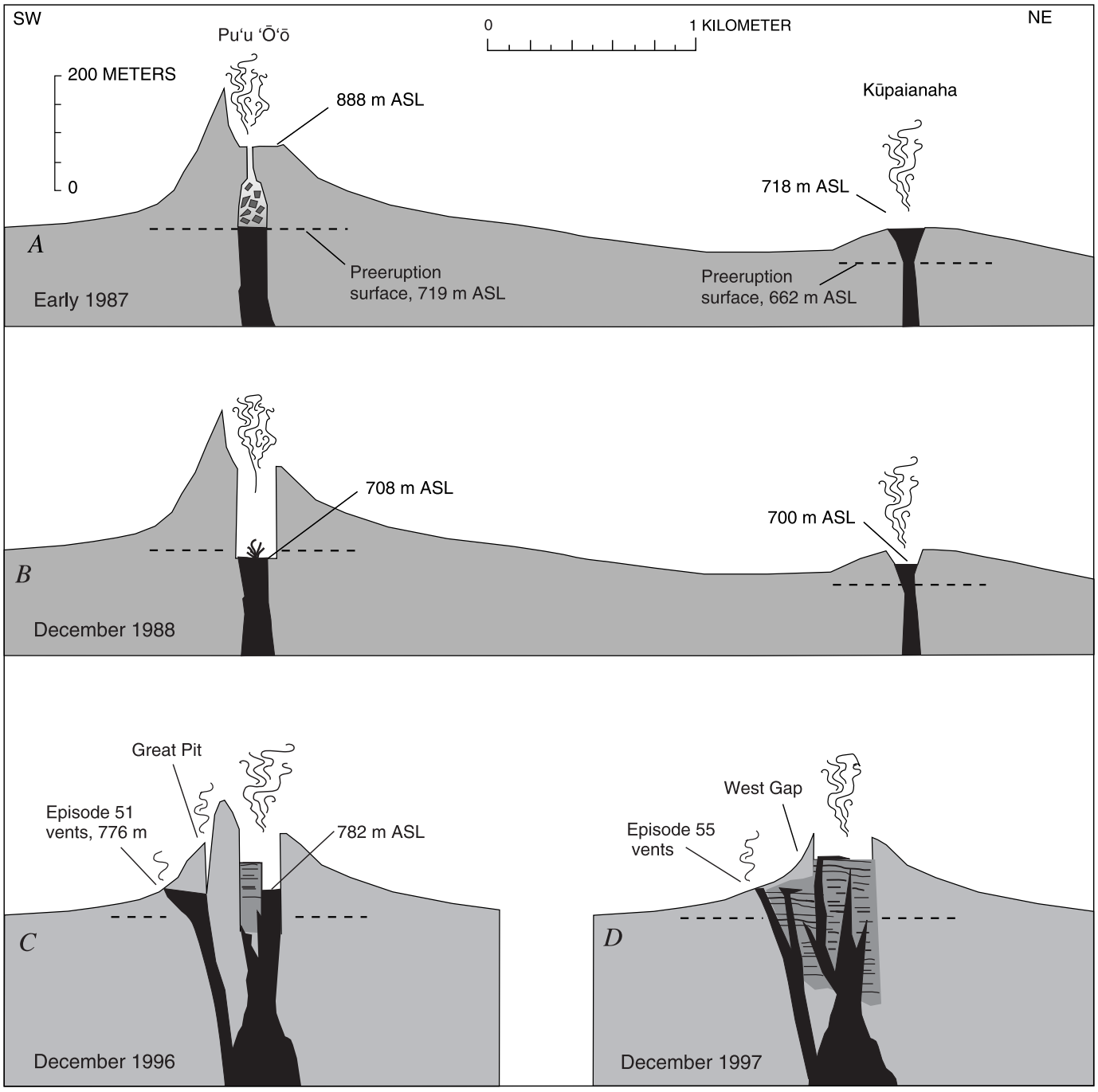

Figure 12. Schematic cross sections showing relative elevations of the Pu‘u ‘Ō‘ō crater floor, flank vents, and Kūpaianaha lava pond. Dashed line, preeruption surface. ASL, above sea level. Vertical exaggeration, 3x. *A*, In July 1986, conduit beneath Pu‘u ‘Ō‘ō fails, and eruption shifts to Kūpaianaha. Pu‘u ‘Ō‘ō is still linked to magma conduit leading from Kīlauea’s summit reservoir to Kūpaianaha. *B*, Collapse of Pu‘u ‘Ō‘ō vent begins in June 1987. Crater stabilizes in December 1988 at 180-m depth below rim. Elevation of lava in crater is nearly the same as that of Kūpaianaha lava pond. *C*, Eruption returns to Pu‘u ‘Ō‘ō in 1992, where radial fissures open on west flank of cone. Great Pit forms upslope of episode 51 vents in 1993 and expands through 1996. *D*, Crater floor and west wall of cone collapse, January 1997. Eruption resumes from episode 55 flank vents on west and south sides of cone.

Date	Crater floor (meters below rim)	Crater floor (meters above sea level)	Crater dimensions (m)	Volume of crater collapse ($10^6 m^3$)	Comments
06/25/87	100	788	30–40	--	
07/24/87	100	788	80*	--	
09/30/87	100	788	120	--	
12/03/87	150	738	150	--	
02/04/88	150	738	150*	--	
08/24/88	--	--	190*	--	
12/31/88	180	690	200	5.6	Cumulative volume of collapse, June 1987–December 1988.
04/30/89	180	690	--	--	
05/18/89	--	--	210*	--	
07/31/89	180	690		--	
08/24/89	180	690	240x210*	--	
12/31/89	180	690	--	--	
08/31/90	80	790	--	--	
12/31/90	80	790	--	--	
06/30/91	80	790	--	--	
08/31/91	40	830	--	--	
10/19/91	36	834	280x240*	--	
11/11/91	120	750	--	3.1	Crater floor collapse, episode 49.
12/23/91	57	809	--	--	
01/24/92	35	831	--	--	
03/27/92	40	826	--	--	
04/16/92	37	829	--	--	
04/24/92	36	830	--	--	
02/08/93	85	781	--	3.1	Crater floor collapse, upper east rift zone intrusion.
02/18/93	--	--	320x240*	--	
02/26/93	60	806	--	--	
10/24/94	--	--	330x240*	--	
09/05/95	60	806	--	--	
02/02/96	57	809	--	--	
06/02/96	--	--	350x240*	--	
12/01/96	60	806	--	--	
01/31/97	210	656	--	13	Crater and west wall collapse, episode 54.
02/24/97	170	696	--	--	
03/21/97	84	782	--	--	
04/01/97	57	809	--	--	
04/18/97	46	820	--	--	
04/29/97	30	836	--	--	
06/16/97	0	866	--	--	Level of pond, not floor. First of 20 crater overflows, averaging about 4 hours, during next 7 months.
07/31/97	45	821	--	--	
10/01/97	45	821	--	--	
01/01/98	30	836	--	--	
01/14/98	0	866	--	--	Level of pond, not floor. Last crater overflow.
02/07/98	30	836	400x240*	--	
03/01/98	30	836	--	--	
06/01/98	35	831	--	--	
10/22/98	40	826	--	--	
04/01/99	55	811	--	--	
09/12/99	120	746	--	<1	Partial crater floor collapse, upper east rift zone intrusion. Estimated depth to collapsed area at center crater.
09/23/99	55	811	--	--	
10/03/99	40	826	400x250*	--	
02/10/00	36	830	--	--	
01/18/01	34	832	--	--	
03/29/02	24	842	--	--	
04/25/02	12	854	--	--	
Total estimated collapse volume ----------				25.8	

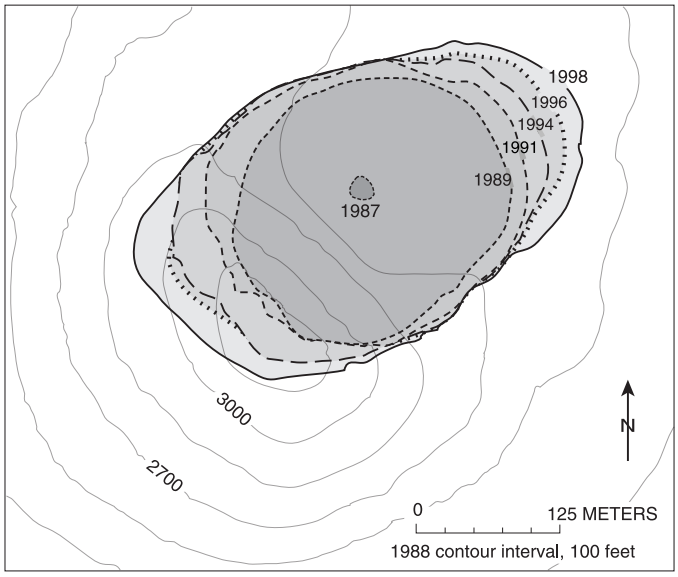

Figure 13. Evolution of the Pu‘u ‘Ō‘ō crater. Crater rims (bold outlines) traced from orthorectified aerial photographs taken from 1987 to 1998. Topographic base (prepared by Ken Hon) shows shape of cone in 1988.

(episode 49) broke out between Pu‘u ‘Ō‘ō and Kūpaianaha (Mangan and others, 1995), and the level of the Pu‘u ‘Ō‘ō lava pond dropped by 30 m. On the fourth day of the eruption, the crater floor collapsed, removing a volume of 3.1×10^6 m^3 (table 3). When the fissure eruption ended after 3 weeks, the lava pond quickly refilled and began resurfacing the talus on the crater floor with fresh pāhoehoe.

In February 1992, the Kūpaianaha vent died. Eleven days later, a radial fissure, 150 m long, opened on the uprift (west) flank of Pu‘u ‘Ō‘ō (episode 50); (Heliker and others, 1998b). Three weeks later, the fissure extended 35 m up the slope of the cone before the flank eruption localized at two main vents (episode 51 vents) at the east end of the fissure. A second fissure, 250 m to the south, was briefly active in late 1992 (episode 52). Three months later, an isolated vent (episode 53 vent) erupted near the end of the episode 52 fissure and was active for the next year.

Central Crater Slowly Widens, 1992–96

From 1992 through 1996, a lava pond was present in the Pu‘u ‘Ō‘ō crater. When full, the pond overflowed and built up the crater floor, which was generally 35 to 60 m below the east rim. The high level of the magma column buttressed the crater walls, and crater expansion was limited to (1) mass wasting of the steep wall beneath the summit and (2) undercutting of the northeast wall by the lava pond, which occupied the northeast end of the crater from January 1991 through April 1995. By these processes, the crater slowly elongated along the trend of the rift zone (fig. 13). The only large collapse of the crater between 1992 and 1996 was triggered by an upper-east-rift-zone intrusion in February 1993, when the lava pond drained and the crater floor collapsed. The volume of this collapse—3.1×10^6 m^3—was about the same as that of November 1991 (table 3).

Flank Vents Undermine Cone, 1992–96

Support for the west wall of the cone was gradually undermined by shallow subsurface magma movement associated with the flank vents. By mid-1992, the episode 51 vents were feeding directly into lava tubes, which rapidly eroded downward through the unconsolidated tephra at the base of the cone. The level of the magma column in the vents dropped in tandem with the downcutting tubes. From 1992 to 1994, the magma column feeding the active flank vents dropped 29 m (Heliker and others, 1998b), and the spatter cones that once marked the vents were consumed by collapse pits. The level of the lava pond within the central crater dropped in concert with the flank vents.

In March 1993, the “Great Pit” formed on the west flank of the cone upslope of the episode 51 flank vents (figs. 14*A*, 14*B*). Lava was intermittently visible at the bottom of the new pit, which probably formed over the east tip of the radial dike that fed the episode 51 vents. The Great Pit enlarged and coalesced with the pits over the episode 51 vents until, by the end of 1996, only a knife-edged ridge separated the composite west-flank pit from the central crater (fig. 14*C*).

Crater Expansion Resumes, Brings Down West Wall of Cone, January 1997

In January 1997, the conduit leading from the summit reservoir to Pu‘u ‘Ō‘ō depressurized as magma was diverted to an intrusion and subsequent fissure eruption (episode 54) in and near Nāpau Crater (fig. 1; Thornber and others, 1997; Owen and others, 2000). In rapid sequence, the Pu‘u ‘Ō‘ō conduit drained, the crater floor collapsed, and part of the cone’s west wall collapsed to leave a gap, 115 m wide (figs. 14*D*, 15). The crater floor dropped approximately 150 m and formed a vertical-walled crater, 210 m deep, with its floor about 65 m below the pre-1983 surface (fig. 16). The January 1997 collapse removed approximately 13×10^6 m^3 of material (table 3) and reduced the height of the cone by 34 m.

The fissure eruption in the Nāpau Crater area lasted only 1 day (Jan. 30–31) and was followed by the longest eruptive hiatus in more than 10 years. Twenty-four days passed before lava rose through the rubble on the floor of the crater, and another 31 days before flank vents resumed erupting.

Cone Burial, 1992–98

Even as the cone was diminished by ongoing collapse, its west and south flanks were being buried beneath the lava shield built by flank vents (fig. 15). The shield grew in several

discrete spurts during periods of eruptive instability (such as the first 6 months of episode 55, in 1997) characterized by shifting vent locations and frequent eruptive pauses. Both of these conditions inhibited lava-tube formation and caused short flows to stack up within 1 km of the vents. About 90 m of the southwest side of the cone disappeared beneath the rising tide of pāhoehoe, while the height of the cone dropped 68 m, owing to collapse.

In June 1997, lava flows poured from the main Pu‘u ‘Ō‘ō crater for the first time since high fountaining ended in 1986. Drain holes in the crater floor periodically clogged, and the lava pond in the crater overflowed the West Gap. Then, 2 months later, lava also overtopped the east rim of the crater, sending flows 1.5 km downrift. These brief spillovers, which continued intermittently through early 1998, plated more of the original cone surface with fresh pāhoehoe (fig. 17).

Southwest Flank Collapse, 1998–Present

A new collapse pit, Puka Nui, formed in December 1997 on the southwest flank of the cone, centered between the rim of the cone and the shield (figs. 18*A,* 18*B*). The pit was initially funnel shaped—50 m in diameter in the loose cinder at the surface, narrowing to 15 to 20 m in width where it intersected layers of agglutinate, with a small, incandescent hole at the bottom. The surface layer of cinder was approximately 20 m deep on this flank, which was along the main trajectory of windborne tephra during the high-fountaining era. As Puka Nui grew, the slope of the cone above the pit slumped into it. Puka Nui quickly assumed the shape of a broad, shallow basin, unlike the Great Pit (fig. 14*B*), where the cinder was not so deep.

Through 1998, Puka Nui expanded rapidly, by coalescing first with a new pit that formed adjacent to it on the slope of the cone, then with pits on the adjacent shield. Collapse slowed in 1999 and 2000, but expansion resumed in 2001 along the eastern margin of the pit. Several spatter cones formed inside Puka Nui during September–October 1999, and fresh lava flows resurfaced the shield part of the pit (fig. 18*C*). As of June 2002, Puka Nui is 180 by 200 m across, and headward erosion of the pit has carved a notch in the rim of the Pu‘u ‘Ō‘ō cone. A zone of circumferential cracks that extends as far as 50 m beyond the pit’s south rim (fig. 19) augurs future collapse.

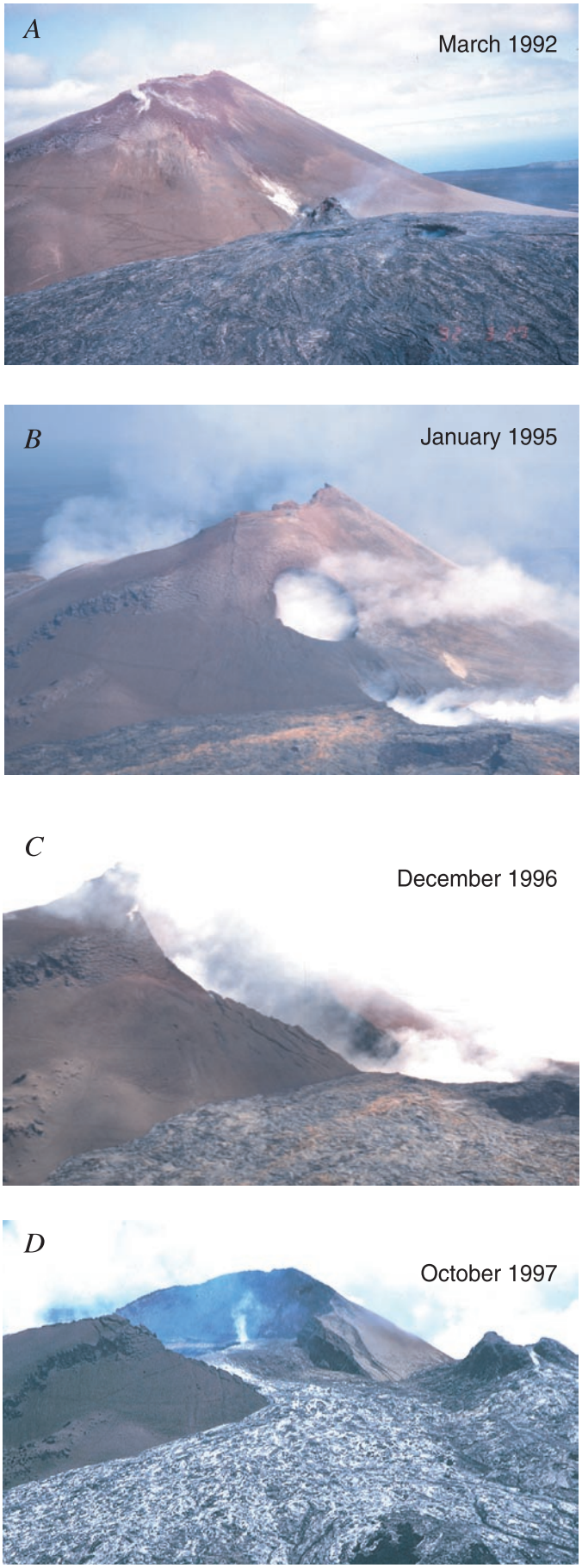

Figure 14. West flank of Pu‘u ‘Ō‘ō. *A*, Spatter cones mark episode 51 vents on west flank of cone in March 1992. *B*, “Great Pit” in January 1995. The pit began to form in early 1993 as flank-vent activity undermined slope. *C*, In December 1996, pits on cone merge with those over episode 51 vents. *D*, By October 1997, the West Gap, formed by January 1997 collapse, is coated by overflows from crater.

Beneath the Cone: the Pu‘u ‘Ō‘ō Plumbing

Previous Work

Previous models of the Pu‘u ‘Ō‘ō magmatic system were predicated on data from the initial 1983 dike emplacement at the beginning of the eruption and from the high-fountaining episodes of 1983–86. In January 1983, a dike linked to the summit reservoir was emplaced in the east rift zone. On the basis of geodetic data, estimates of the dike's dimensions ranged from ~2 to 3.5 m wide, 11.4 to 15 km long, and 2.4 to 4.4 km high (Dvorak and others, 1986; Okamura and others, 1988; Hall Wallace and Delaney, 1995). Seismicity associated with dike emplacement was centered about 2.5 km beneath Makaopuhi (fig. 1), deepening to 3.5 km below Kalalua (Klein and others, 1987). The dike ascended to intersect the surface along a 7.5-km stretch of the rift zone from Nāpau Crater to Kalalua (Wolfe and others, 1987).

After the eruption became localized at Pu‘u ‘Ō‘ō, Wolfe and others (1987, 1988) postulated that the vent was connected to the original dike by a vertical, cylindrical pipe, 38 to 66 m in diameter in its upper 1,000 m. This model, based on the volume of gas-enriched melt erupted during the highest fountains early in an episode, assumed that gas accumulates in the upper 1,000 m of the pipe. Greenland and others (1988) calculated a similar diameter (50 ±30 m) for a cylindrical pipe about 2,200 m high, on the basis of both SO_2 emissions and summit inflation during repose periods. They also calculated a volume range of 7–11x10^6 m^3 for the pipe.

Hoffmann and others (1990) used near-vent deformation measurements during high-fountaining episodes to model the shallow magma reservoir beneath Pu‘u ‘Ō‘ō as a tabular body, 2.5 km high, 1.6 km long, and 2.5 to 3 m wide, with a volume of 10 x10^6 to 12x10^6 m^3. They inferred the top of this modeled dike to be 400 m below the surface and postulated that the dike was linked to the surface by a cylindrical conduit, 20 m in diameter.

Wilson and Head (1988) argued that the shallow plumbing of Pu‘u ‘Ō‘ō, at more than a few hundred meters depth, must be planar and less than a few meters wide. They proposed, on the basis of fluid dynamics of the high-fountaining episodes, that a shallow tabular body, about 3.5 m wide, 1 km high, and 100 m long, with a volume of 7.5x10^5 m^3, was linked to the surface by a cylindrical conduit, 10 m in diameter and no more than a few hundred meters high.

In 1988, while Kūpaianaha was the active vent, Goldstein and Chouet (1994) deployed a dense array of seismometers near Pu‘u ‘Ō‘ō to model the source of volcanic tremor recorded near the cone. They determined that the tremor sources were beneath, or in close proximity to, Pu‘u ‘Ō‘ō, within an area about 400 m in diameter. They concluded that these sources, which could be resonating fluid-filled cracks or point sources, such as exploding gas bubbles in magma, were located mainly within a few hundred meters of the surface.

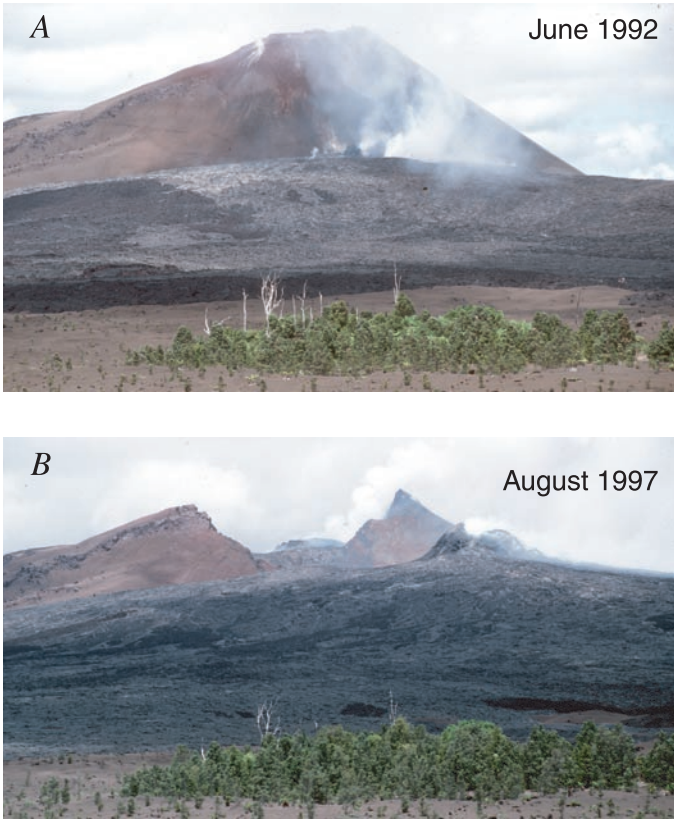

Figure 15. Pu‘u ‘Ō‘ō cone in June 1992 (*A*) and August 1997 (*B*), after collapse of west wall of cone and growth of episodes 50–55 shield. Spatter cones on shield mark episode 51 (1992) and episode 55 (1997) flank vents. Photograph in figure 15*A* taken by T.N. Mattox.

New Geophysical Evidence

Geodetic Data

In February 1999, a borehole tiltmeter (sta. POO; fig. 20*A*) was installed 1.9 km northwest of the Pu‘u ‘Ō‘ō crater. During steady eruption, this tiltmeter rarely records any changes greater than the diurnal variation in the signal. The tiltmeter has responded, however, to several short-term magmatic events, including upper-east-rift-zone intrusions and pauses in the eruption. During such events, the station POO tiltmeter generally tracked the borehole tiltmeter at Kīlauea's summit, recording inflation of the rift zone during pauses, and deflation as the eruption resumed. During the largest events recorded by station POO (the Sept. 11, 1999, and Feb. 23, 2000, intrusions), the tilt vectors pointed to a source 1.5 to 2.3 km uprift from the center of the crater (fig. 20*A*), presumably the dike leading from the summit to Pu‘u ‘Ō‘ō.

In January 2000, another borehole tiltmeter (sta. POC; fig. 20*A*) was installed on the northwest flank of the Pu‘u ‘Ō‘ō cone at about the elevation of the crater floor. This tiltmeter has proved highly responsive to short-term magmatic events, including the February 2000 upper-east-rift-zone intrusion and

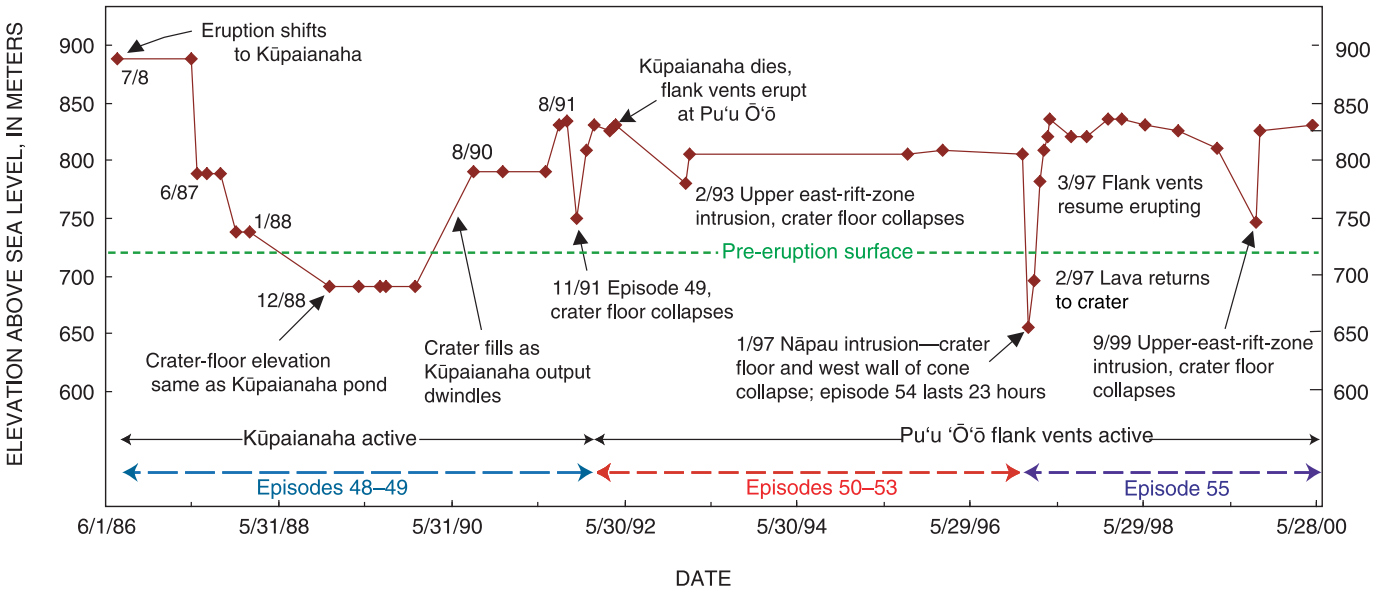

Figure 16. Timeline of Pu'u 'Ō'ō crater formation, showing crater-floor elevations from June 1986 to June 2000. Elevation of crater floor did not change significantly from June 2000 through end of 2001.

several pauses and surges in effusion rate. During such events, the azimuth of tilt ranges from 132° to 149°, pointing just west of the center of the crater. Most of the magmatic events recorded at station POC are not detected by the more distant station POO tiltmeter, which indicates that the deformation source at Pu'u 'Ō'ō is both local and shallow—probably less than 400 m below the preeruption surface.

In April 2002, a third tiltmeter (sta. POS; fig. 20*A*) was installed on the northeast flank of Pu'u 'Ō'ō, just in time to record a large magmatic event that produced a surge in effusion rate at Pu'u 'Ō'ō. The results of modeling the data from the two tiltmeters on the cone suggest a radially symmetric deformation source, approximately 250 m below the preeruption surface.

The station POC tiltmeter has recorded not only rapid tilt changes in response to short-lived magmatic events, but also long-term, quasi-steady tilting down toward the eastern side of the crater. The long-term tilt signal is corroborated by a continuously recording, single-frequency (L1) Global Positioning System (GPS) receiver installed on the northwest flank of Pu'u 'Ō'ō in 1999 (sta. L1; fig. 20*A*). The L1 station data for 2000–01 show approximately 9 cm/yr of steady subsidence relative to another GPS receiver located near the station POO tiltmeter.

A set of bench marks along the east rift zone at the Pu'u 'Ō'ō cone was surveyed in January 1998 and April 2002, using kinematic GPS and total-station methods. Vertical precision is better than 5 cm for the GPS survey and better than 1 cm for the total station data. For illustrative purposes, the along-rift locations are projected onto a line and referenced by their distance from pin 4 at the northeast end of the line (fig. 20*A*). Cumulative subsidence over the 4.3-year interval increases toward the cone and ranges from 63 to 83 cm in the crater area (north spillway to sta. L1, fig. 20*B*), corresponding to an average subsidence rate of 16 to 21 cm/yr. Maximum observed subsidence of 193 cm was found in the West Gap, an area of highly broken ground that has had a complex subsidence pattern since cone collapse in January 1997.

The long-term subsidence recorded by the two surveys and by the continuously recording instruments on the cone probably results from a combination of causes, including the cone settling under its own weight, gravitational failure of the cone's flanks, and long-term subsidence of the rift zone.

Gravity Data

Between January 1998 and February 2000, more than 100 gravity measurements—including 4 on the crater floor—were made at 84 stations within a 2-km radius of the Pu'u 'Ō'ō crater (fig. 21*A*). The elevation of each site was determined by using a combination of differential GPS measurements and total-station surveying; vertical precision ranged from 1 to 5 cm. The gravity measurements have a typical error of 25 to 30 μGal and were reduced to a standard free-air anomaly.

The densities of the cone and the surrounding lava flows erupted since 1983 are probably lower than those of most Hawaiian rocks. Detailed knowledge of the topography and density of these deposits was needed to further reduce the data to reveal subsurface structures. In 1999, much of Pu'u 'Ō'ō was surveyed with the total-station instrument. The results of the survey were used in conjunction with aerial photographs to produce a topographic map (fig. 17). The topography of areas outside this map was estimated from site elevations by using the 1993 radar DEM data of Rowland and others (1999) as a guide.

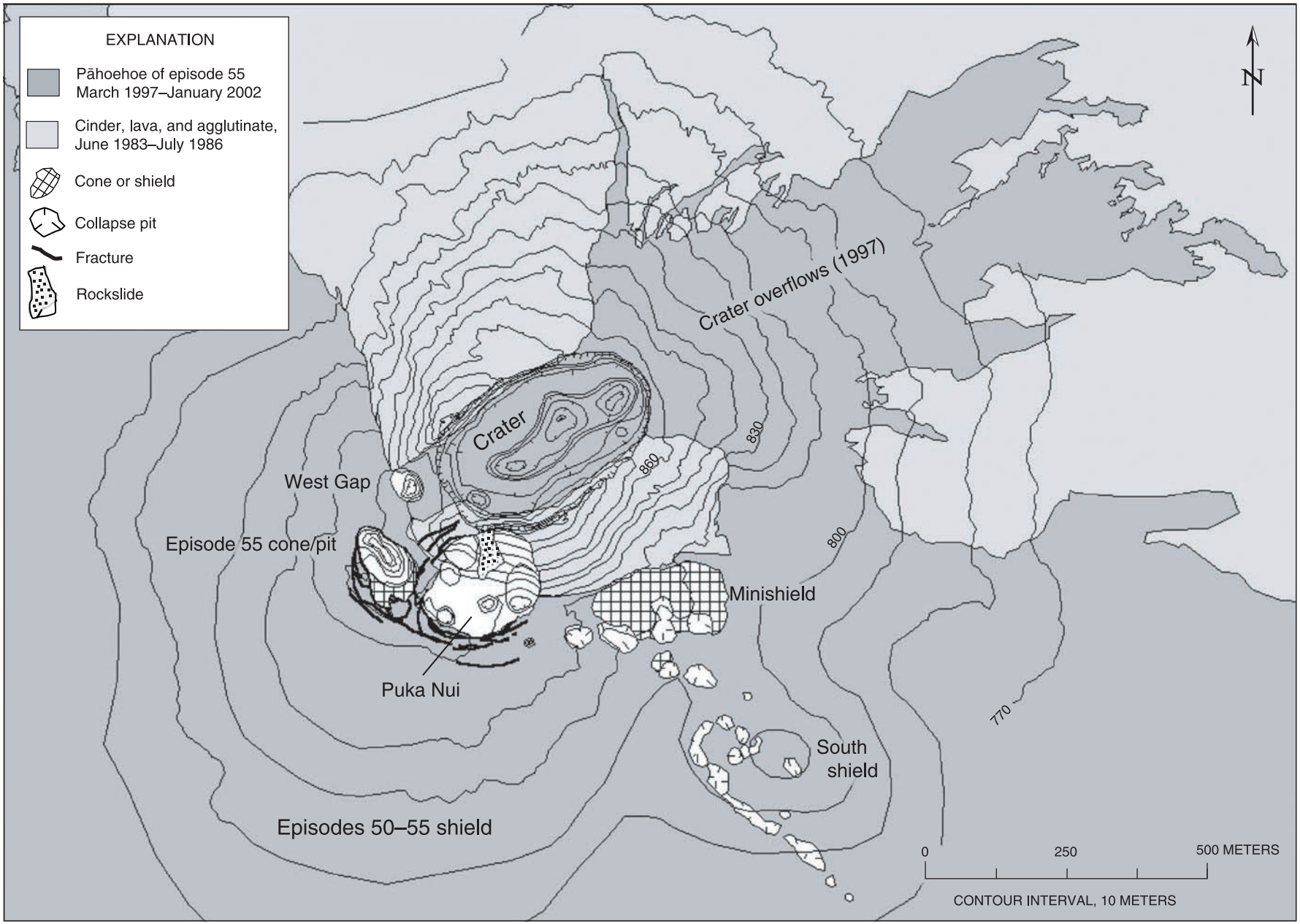

Figure 17. Map of the Pu‘u ‘Ō‘ō cone. Contours from topographic survey in 1999, using total-station data in conjunction with aerial photographs. Contours inside crater and collapse pits as of July 2001.

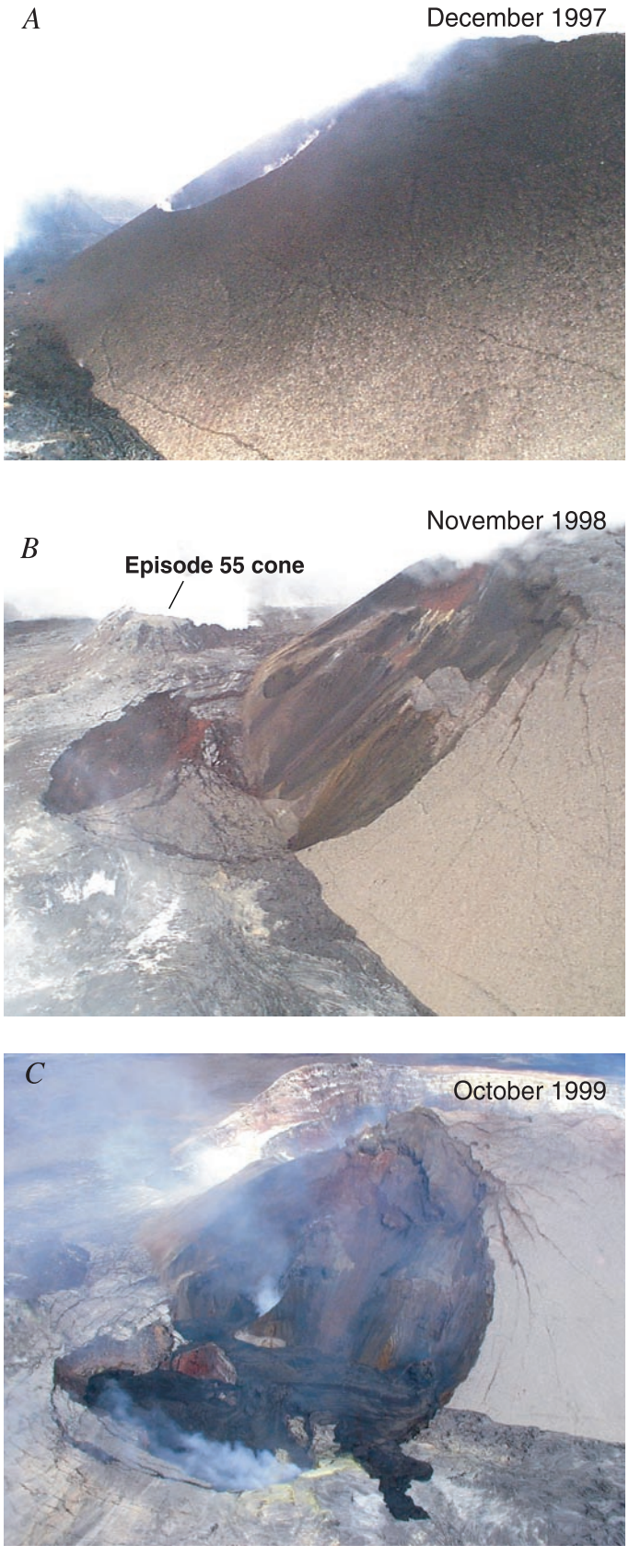

Figure 18. Southwest flank of Pu‘u ‘Ō‘ō. *A*, In December 1997, Puka Nui forms high on flank of cone. *B*, In November 1998, composite pit expands and merges with pits undermining adjacent shield. *C*, In September–October 1999, four spatter cones form inside pit, which partly fills with pāhoehoe. Small tongue of black pāhoehoe spills out of pit on lower right.

An average density of 1.50 g/cm^3 was estimated for the Pu‘u ‘Ō‘ō cone by computing the proportional density contribution from the tephra, lava flow, and agglutinate units (table 2). A density of 2.0 g/cm^3 was assumed for the shield lava flows that mantle the west and south flanks. We used these densities and the above-derived topography to compute the cone's gravitational response with the USGS computer program GRAVPOLY (Godson, 1983). The residual values computed from the formula

residual = free-air anomaly - (1.50 g/cm^3 [cone] + 2.0 g/cm^3 [shield])

are mapped in figure 21*A*. The isogal contours define two features: a chevron pattern pointing east-northeastward downrift and a narrow, oblong trough of low residuals centered over the crater south of the chevron ridge axis. The chevron pattern is an expression of the general rift-zone gravity high (see Kauahikaua and others, 2000, fig. 2). We interpret the trough to be a low-density zone, approximately 500 m wide and 1,500 m long (fig. 21*B*).

One model we can use to explain the trough is a body with a density contrast of -0.5 g/cm^3 in a volume 300 m thick, between 350 m and 650 m above sea level (70–370 m below the preeruption surface). The modeled depth range is not unique but is consistent with the shallow deformation source indicated by the tiltmeter data. The low-density zone lies within pre-Pu‘u ‘Ō‘ō lava flows—assumed to have a density of approximately 2.0 g/cm^3—giving an estimated model density of 1.5 g/cm^3.

Discussion

The Shallow Plumbing System

Roche and others (2001), in recent experimental work on crater-collapse mechanisms, modeled collapse over an underpressurized magma reservoir. In experiments using roof-aspect ratios (roof thickness/roof width) >1, they found that the initial subsidence is subsurface and noncoherent; that is, "chaotic stoping accompanies intense brecciation of the reservoir roof." Subsurface collapse over a cylindrical reservoir left a cavity capped by a stable roof. With continued subsidence, the cavity migrated upward until the surface abruptly collapsed. In their experimental model, the end result was a crater underlain by a cylinder of brecciated material occupying about twice the volume of the same material before collapse. By analogy, we can expect that, in the aftermath of the January 1997 collapse, an elongate volume of brecciated rock underlies the crater and the west wall of the cone.

The low-density trough inferred from the gravity map probably represents brecciated rock, created by repeated cone collapse, riddled with magma-filled fractures. The brecciated

rock beneath the cone originally had a density of 1.5 to 2.0 g/cm^3. If it now takes up twice its original volume, its density would be halved. In the depth range 70–370 m below the base of the cone, magma averages about 70 percent bubbles and has a density of ~0.8 g/cm^3 (Mangan and others, 1993).

The volume of material lost during the January 1997 collapse, 13x10^6 m^3, gives us a minimum for the current size of the shallow magma system at Pu‘u ‘Ō‘ō. Data from tiltmeters near and on the cone indicate that the deformation source is less than 400 m below the preeruption ground surface, with a deeper source 1.5 to 2.3 km uprift of the crater (fig. 20*A*). These observations weigh against the notion of a vertical conduit, about 50 m in diameter, extending ≥1,000 m below the crater, as postulated in earlier studies (for example, Wolfe and others, 1988). Such a conduit would probably produce a much greater tilt signal than we observe. Although the geometry of the deformation source beneath the cone remains unclear in detail, models based on tiltmeter data suggest that the source is more likely radially symmetrical than tabular.

Changing Vent Distributions

The January 1997 collapse caused significant changes in the subsurface plumbing that were reflected in the distribution of flank vents. From 1992 through 1996 (episodes 50–53), the flank vents evolved from eruptive fissures aligned along the trace of the rift zone or subparallel to it (Heliker and others, 1998b). When episode 55 began, after the January 1997 collapse, the first flank vent to erupt was at the base of the newly formed West Gap, close to the pre-collapse vents. Thereafter, eruptive activity quickly migrated southward around the cone, with lava effusion shifting back and forth among four to six vents that were not aligned along fissures (fig. 22).

As these early episode 55 vents were erupting, we debated whether they were true vents fed from below the preeruption ground surface, or rootless vents fed by a deep tube leading from vents at the base of the West Gap. No links between any of the episode 55 vents were detected by very low frequency

Figure 19. Southwest flank of Pu‘u ‘Ō‘ō and collapse features. Dashed line encloses composite collapse pit, Puka Nui; another collapse pit engulfs episode 55 cone. Concentric cracks on shield extend well beyond present pits. Photograph taken by R.P. Hoblitt on February 7, 2002.

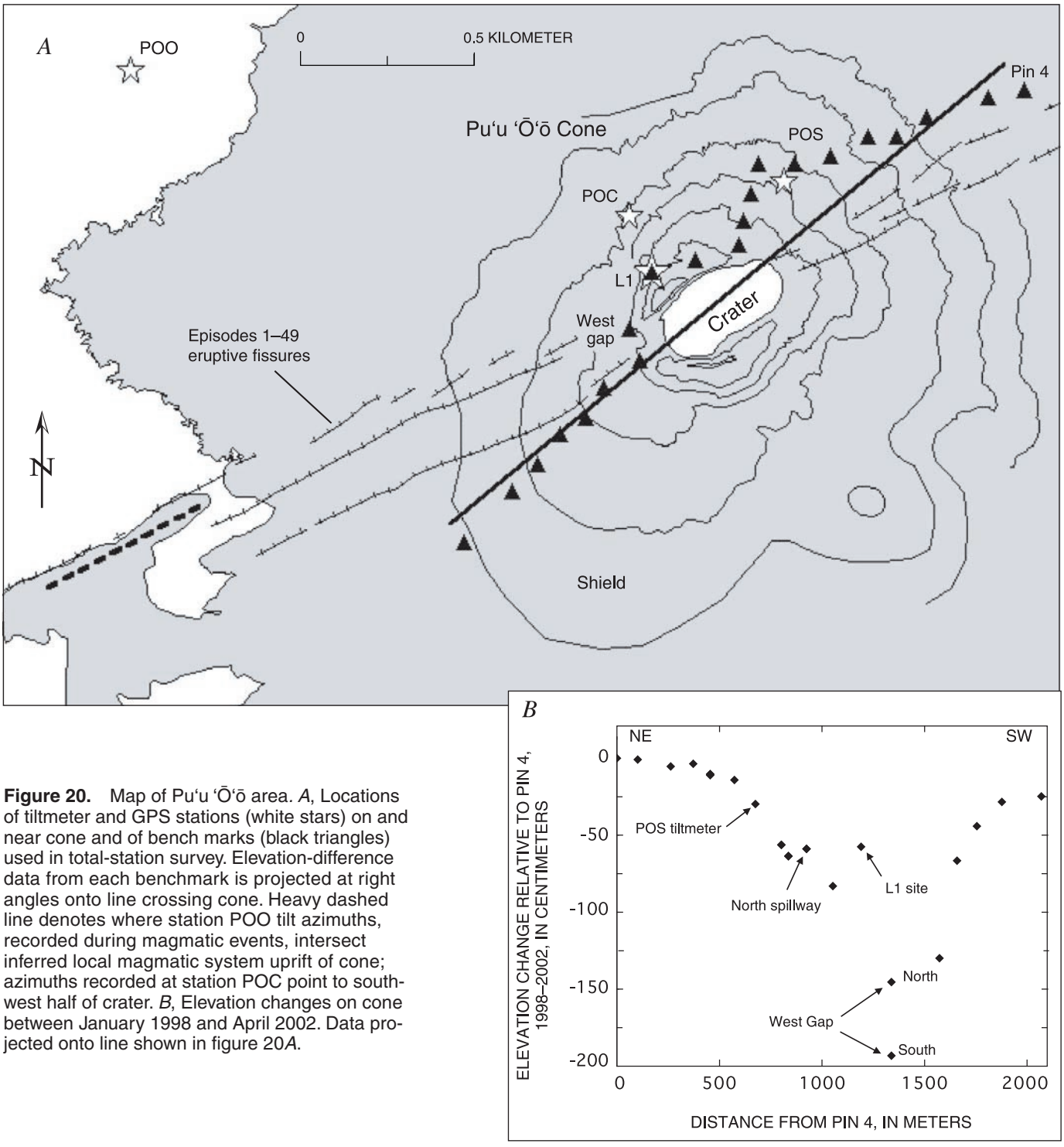

Figure 20. Map of Pu‘u ‘Ō‘ō area. *A*, Locations of tiltmeter and GPS stations (white stars) on and near cone and of bench marks (black triangles) used in total-station survey. Elevation-difference data from each benchmark is projected at right angles onto line crossing cone. Heavy dashed line denotes where station POO tilt azimuths, recorded during magmatic events, intersect inferred local magmatic system uprift of cone; azimuths recorded at station POC point to southwest half of crater. *B*, Elevation changes on cone between January 1998 and April 2002. Data projected onto line shown in figure 20*A*.

(VLF) measurements, a geoelectrical technique that can detect lava tubes a few tens of meters below the surface (Kauahikaua and others, 1996). Yet within a year, a string of collapse pits in the episodes 50–55 shield linked the West Gap with the uppermost detectable part of the lava tube feeding surface flows (figs. 19, 22). Incandescence and, rarely, moving lava have been glimpsed at the bottom of these collapse pits, but none has had the appearance of a normal skylight over a tube containing a fast-moving stream of lava.

In September–October 1999, in response to heightened pressure in the magmatic system after an 11-day pause in the eruption, five spatter cones formed within collapse pits on the southwest flank of the cone (fig. 22). Two of the spatter cones in Puka Nui arose from the collapsed wall of the Pu‘u ‘Ō‘ō cone, rather than from the shield, and so were clearly not connected to any existing lava tube.

These observations lead us to conclude that the episode 55 vents are fed by one or more dikes rather than by a shallow

lava tube. The distribution of these vents indicates that dike emplacement beneath the cone, at least at shallow levels, is no longer controlled by the tensional regime parallel to the rift zone. The arcuate trend of episode 55 vents suggests that their position is controlled by deep, concentric fracturing on the west side of the cone resulting from the catastrophic collapse of January 1997.

The distribution of vents inside the crater also was permanently disrupted by the January 1997 collapse. The lava pond that was almost continuously active from 1990 through 1996 was replaced by a succession of vents on the crater floor, apparently because the central conduit that had long fed the crater was blocked by rubble and replaced by multiple feeders.

Future Outlook for Pu‘u ‘Ō‘ō

As of mid-2002, the Pu‘u ‘Ō‘ō cone continues to collapse. Flank-vent activity on the southwest side of the cone is ongoing, and the composite collapse pit, Puka Nui, is enlarging. Another event that depressurizes the magmatic system beneath Pu‘u ‘Ō‘ō, as did the January 1997 intrusion, is almost certain to trigger collapse of the southwest wall of the cone.

To date, the cone has lost 27 percent of its original height because of collapse. On the south and west flanks, the lower third of the cone has disappeared beneath the lava shield created by multiple flank vents. If the eruption continues in the

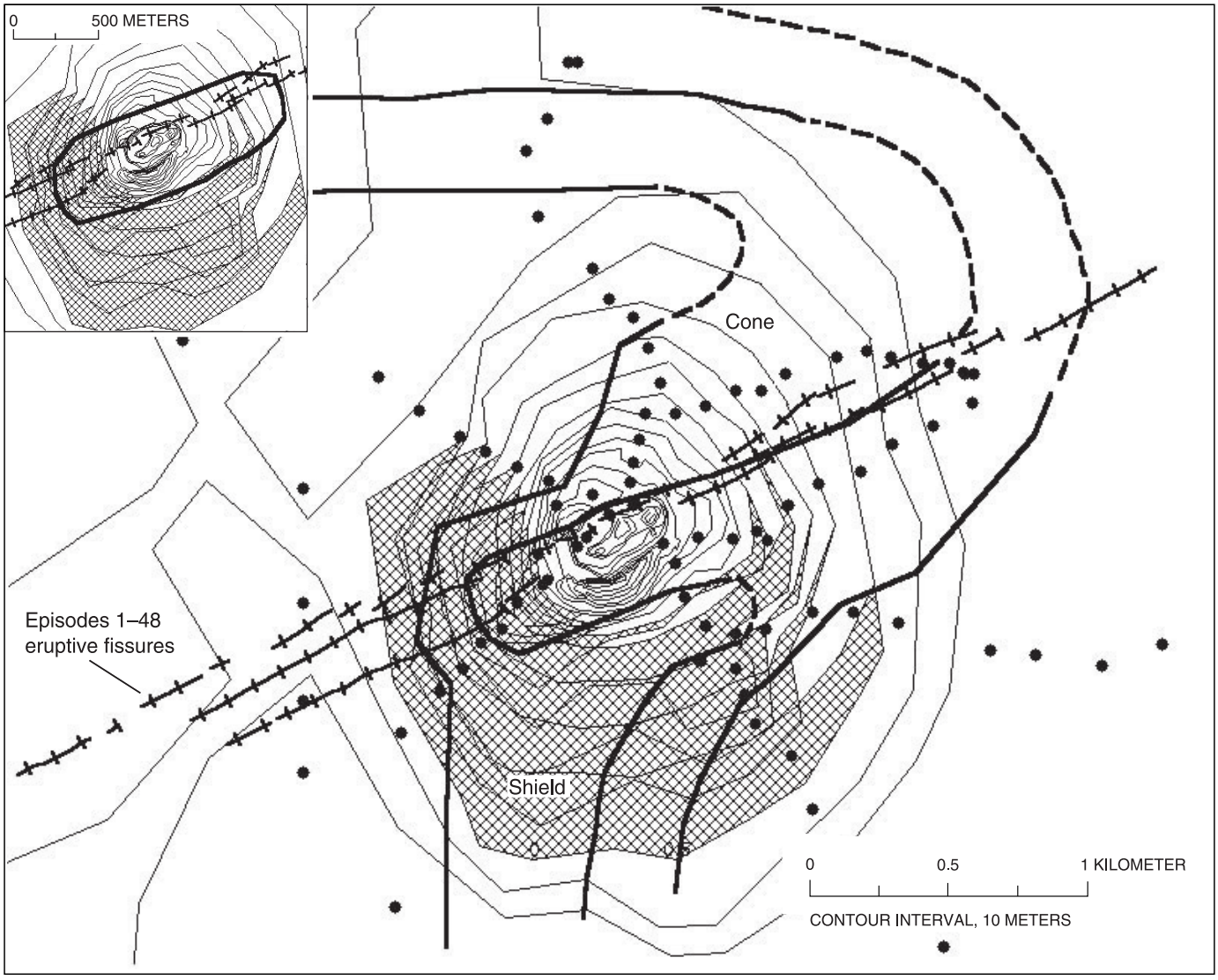

Figure 21. Gravity data on the Pu‘u ‘Ō‘ō cone and adjacent shield. Generalized 10-m elevation contours (thin lines) subdivided to assign different densities for modeling purposes. Shield is distinguished from cone by stippling. GRAVPOLY software-computed gravitational attraction model is made up of 10-m-thick slabs with vertical edges. Thick lines are 1-mGal contours of free-air anomaly minus gravitational attraction of cone (1.5 g/cm^3) and shield (2.0 g/cm^3), dashed where inferred. *Inset*, Oblong outline centered on Pu‘u ‘Ō‘ō is boundary of modeled low-density area suggested by pattern of gravity contours.

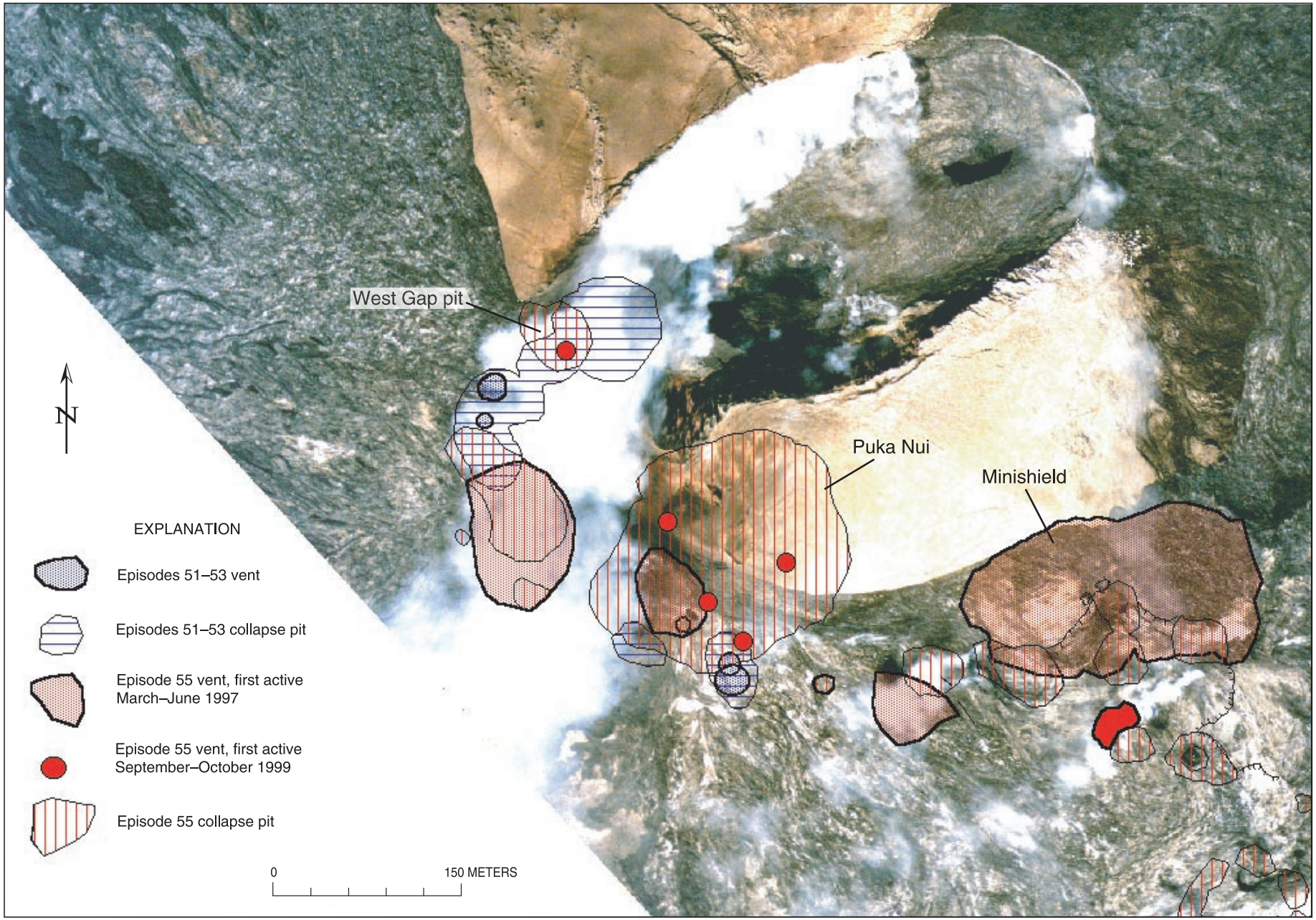

Figure 22. Episodes 51–55 vents and collapse pits on west and south flanks of Pu‘u ‘Ō‘ō superimposed on orthorectified aerial photograph taken February 1998.

same mode, Pu‘u ‘Ō‘ō will eventually evolve into a low shield with a compound crater formed by coalescence of the central-vent crater and the collapse pits on the southwest slope of the cone. The cone’s foundation of tephra, lava, and agglutinated spatter will be obscured by an overplating of pāhoehoe from crater overflows and flank vents.

Acknowledgments

We gratefully acknowledge the expertise and opinions shared by our colleagues, past and present, at the Hawaiian Volcano Observatory (HVO) and the able assistance supplied by countless volunteers and student workers. Former staff geologists George Ulrich, Ken Hon, Margaret Mangan, Tari Mattox, and Carl Thornber all contributed to collecting the data and making the interpretations presented here. Discussions in the field with Don Swanson and Maya Yasui were helpful in clarifying our thoughts about rootless spatter flows. We thank Robert Tilling and Richard Hoblitt for their careful reviews of the manuscript. During the 2 decades of this eruption, HVO has relied heavily on the exceptional skills of two helicopter pilots, David Okita and Bill Lacey III, whom we thank for all their contributions to our work.

References Cited

Dvorak, J.J., Okamura, A.T., English, T.T., Koyanagi, R.Y., Nakata, J.S., Sako, M.K., Tanigawa, W.R., and Yamashita, K.M., 1986, Mechanical response of the south flank of Kilauea volcano, Hawaii, to intrusive events along the rift systems: Tectonophysics, v. 124, no. 3–4, p. 193–209.

Elias, Tamar, Sutton, A.J., Stokes, J.B., and Casadevall, T.J., 1998, Sulfur dioxide emission rates of Kilauea Volcano, Hawaii, 1979–1997: U.S. Geological Survey Open-File Report 98–462, 40 p.

Godson, R.H., 1983, GRAVPOLY; a modification of a three-dimensional gravity modelling program: U.S. Geological Survey Open-File Report 83–346, 53 p.

Goldstein, Peter, and Chouet, B.A., 1994, Array measurements and modeling of sources of shallow volcanic tremor at Kilauea Volcano, Hawaii: Journal of Geophysical Research, v. 99, no. B2, p. 2637–2652.

Greenland, L.P., Okamura, A.T., and Stokes, J.B., 1988, Constraints on the mechanics of the eruption, chap. 5 *of* Wolfe, E.W., ed., The Puu Oo eruption of Kilauea Volcano, Hawaii; episodes 1 through 20, January 3, 1983, through June 8, 1984: U.S. Geological Survey Professional Paper 1463, p. 155–164.

Hall Wallace, M.K., and Delaney, P.T., 1995, Deformation of Kilauea volcano during 1982 and 1983; a transition period: Journal of Geophysical Research, v. 100, no. B5, p. 8201–8219.

Head, J.W., III, and Wilson, Lionel, 1989, Basaltic pyroclastic eruptions; influence of gas-release patterns and volume fluxes on fountain structure, and the formation of cinder cones, spatter cones, rootless flows, lava ponds and lava flows: Journal of Volcanology and Geothermal Research, v. 37, no. 3–4, p. 261-271.

Heliker, C.C., Mangan, M.T., Mattox, T.N., and Kauahikaua, J.P., 1998a, The Puʻu ʻŌʻō-Kūpaianaha eruption of Kīlauea, November 1991–February 1994; field data and flow maps: U.S. Geological Survey Open-File Report 98–103, 10 p., 2 sheets, scale 1:50,000.

Heliker, C.C., Mangan, M.T., Mattox, T.N., Kauahikaua, J.P., and Helz, R.T., 1998b, The character of long-term eruptions; inferences from episodes 50–53 of the Pu‘u ‘Ō‘ō-Kūpaianaha eruption of Kīlauea Volcano: Bulletin of Volcanology, v. 59, no. 6, p. 381–393.

Hoffmann, J.P., Ulrich, G.E., and Garcia, M.O., 1990, Horizontal ground deformation patterns and magma storage during the Puu Oo eruption of Kilauea volcano, Hawaii; episodes 22–42: Bulletin of Volcanology, v. 52, no. 6, p. 522–531.

Kauahikaua, J.P., Hildenbrand, T.G., and Webring, M.W., 2000, Deep magmatic structures of Hawaiian volcanoes, imaged by 3D gravity models: Geology, v. 28, no. 10, p. 883–886.

Kauahikaua, J.P., Mangan, M.T., Heliker, C.C., and Mattox, T.N., 1996, A quantitative look at the demise of a basaltic vent; the death of Kupaianaha, Kilauea Volcano, Hawai‘i: Bulletin of Volcanology, v. 57, no. 8, p. 641–648.

Klein, F.W., Koyanagi, R.Y., Nakata, J.S., and Tanigawa, W.R., 1987, The seismicity of Kilauea’s magma system, chap. 43 *of* Decker, R.W., Wright, T.L., and Stauffer, P.H., eds., Volcanism in Hawaii: U.S. Geological Survey Professional Paper 1350, v. 2, p. 1019–1185.

Mangan, M.T., Cashman, K.V., and Newman, Sally, 1993, Vesiculation of basaltic magma during eruption: Geology, v. 21, no. 2, p. 157–160.

Mangan, M.T., Heliker, C.C., Mattox, T.N., Kauahikaua, J.P., and Helz, R.T., 1995, Episode 49 of the Pu‘u ‘O‘o-Kupaianaha eruption of Kilauea volcano—breakdown of a steady-state eruptive era: Bulletin of Volcanology, v. 57, no. 2, p. 127–135.

Okamura, A.T., Dvorak, J.J., Koyanagi, R.Y., and Tanigawa, W.R., 1988, Surface deformation during dike propagation, chap. 6 *of* Wolfe, E.W., ed., The Puu Oo eruption of Kilauea Volcano, Hawaii; episodes 1 through 20, January 3, 1983, through June 8, 1984: U.S. Geological Survey Professional Paper 1463, p. 165–182.

Owen, S.E., Segall, Paul, Lisowski, Michael, Miklius, Asta, Murray, Michael, Bevis, M.G., and Foster, James, 2000, January 30, 1997 eruptive event on Kilauea Volcano, Hawaii, as monitored by continuous GPS: Geophysical Research Letters, v. 27, no. 17, p. 2757–2760.

Roche, Olivier, van Wyk de Vries, Benjamin, and Druitt, T.H., 2001, Sub-surface structures and collapse mechanisms of summit pit craters: Journal of Volcanology and Geothermal Research, v. 105, no. 1, p. 1–18.

Rowland, S.K., MacKay, M.E., and Garbeil, Harold, 1999, Topographic analyses of Kīlauea Volcano, Hawai‘i, from interferometric airborne radar: Bulletin of Volcanology, v. 61, no. 1, p. 1–14.

Smith, G.A., Florence, P.S., Castrounis, M.L., Luongo, Mark, Moore, J.D., Throne, John, and Zelley, Karin, 1999, Basaltic

near-vent facies of Vulcan cone, Albuquerque volcanoes, New Mexico, *in* Pazzaglia, F.J., and Lucas, S.G., Albuquerque geology: New Mexico Geological Society Guidebook, v. 50, p. 211–219.

Sparks, R.S.J., and Pinkerton, Harry, 1978, Effect of degassing on rheology of basaltic lava: Nature, v. 276, no. 5686, p. 385–386.

Sumner, J.M., 1998, Formation of clastogenic lava flows during fissure eruption and scoria cone collapse; the 1986 eruption of Izu-Oshima Volcano, eastern Japan: Bulletin of Volcanology, v. 60, no. 3, p. 195–212.

Thornber, C.R., Sherrod, D.R., Heliker, C.C., Kauahikaua, J.P., Trusdell, F.A., Lisowski, Michael, and Okubo, P.G., 1997, Kilauea's ongoing eruption; Nāpau Crater revisted after 14 years [abs.]: Eos (American Geophysical Union Transactions), v. 78, no. 17, supp., p. S329.

Wilson, Lionel, and Head, J.W., III, 1988, Nature of local magma storage zones and geometry of conduit systems below basaltic eruption sites; Puʻu ʻOʻo, Kilauea east rift, Hawaii, example: Journal of Geophysical Research, v. 93, no. B12, p. 14785–14792.

Wolfe, E.W., Garcia, M.O., Jackson, D.B., Koyanagi, R.Y., Neal, C.A., and Okamura, A.T., 1987, The Puu Oo eruption of Kilauea Volcano, episodes 1–20, January 3, 1983, to June 8, 1984, chap. 17 *of* Decker, R.W., Wright, T.L., and Stauffer, P.H., eds., Volcanism in Hawaii: U.S. Geological Survey Professional Paper 1350, v. 1, p. 471–508.

Wolfe, E.W., Neal, C.A., Banks, N.G., and Duggan, T.J., 1988, Geologic observations and chronology of eruptive events, chap. 1 *of* Wolfe, E.W., ed., The Puu Oo eruption of Kilauea Volcano, Hawaii; episodes 1 through 20, January 3, 1983, through June 8, 1984: U.S. Geological Survey Professional Paper 1463, p. 1–97.

Wolff, J.A., and Sumner, J.M., 2000, Lava fountains and their products, *in* Sigurdsson, Haraldur, Houghton, B.F., McNutt, S.R., Rymer, Hazel, and Stix, John, eds., Encyclopedia of volcanoes: San Diego, Calif., Academic Press, p. 321–329.